

Buyang Huanwu Decoction Alleviates Cerebral Ischemia-Reperfusion Injury via Sirtuin 1/Autophagy Pathway

Han Li

Guangzhou University of Chinese Medicine

Xin-Yi Lu

Guangzhou University of Chinese Medicine

Dong Peng

Guangzhou University of Traditional Chinese Medicine First Affiliated Hospital

Yang Zhang

Guangzhou University of Chinese Medicine

Hao Lin

Guangzhou University of Chinese Medicine

Shi-Jie Zhang (✉ shijiezhang@gzucm.edu.cn)

Guangzhou University of Chinese Medicine

Li Guan

Guangzhou University of Chinese Medicine

Research

Keywords: Buyang Huanwu Decoction, ischemia-reperfusion, SIRT1, autophagy

Posted Date: November 12th, 2020

DOI: <https://doi.org/10.21203/rs.3.rs-104132/v1>

License: © ⓘ This work is licensed under a Creative Commons Attribution 4.0 International License.

[Read Full License](#)

Abstract

Background

Stroke accounts for a large proportion of deaths from disease around world. Buyang Huanwu Decoction (BHD) is used to protect against stroke and stroke-induced disability for many years in China. However, the mechanism of BHD to protect against stroke is still confused.

Methods

The middle cerebral artery occlusion and reperfusion (MCAO-R) model was used to investigate in this study. The animals were administrated with BHD (5, 10 and 20 g/kg) or rapamycin respectively. Infarct size and modified neurological severity score (mNSS) on day 5 were calculated. Cellular changes around ischemic penumbra were showed by HE staining and Nissl staining. Protein expressions of nestin, brain-derived neurotrophic factor (BDNF), doublecortin on the X-chromosome (DCX) and autophagy-related protein in the cerebral peri-ischemic area were detected.

Results

In results, the post-treatment with BHD relieved brain infarct size and improved neurological deficits in MCAO-R rats. BHD protected against MCAO-R-induced neuronal necrosis, obviously enhanced autophagy (increased Beclin 1 and LC3, decreased P62) and increased the protein expressions of nestin, BDNF and DCX. Meanwhile, BHD promoted the expression of Sirtuin1/SIRT1, an important regulator of autophagy.

Conclusions

In conclusion, our data suggested that post-treatment with BHD could protect rat brain from ischemia-reperfusion injury via SIRT1/autophagy pathway.

Background

Recently years, stroke has become one of the most common causes of death around the world. It has been the fifth leading cause of death from disease in western country but the second leading cause in China during the past 10 years (Benjamin et al. 2018, Zhou et al. 2016). Stroke occurred when the brain blood supply interrupted or reduced, which prevents brain tissue from getting oxygen and nutrients (Feigin et al. 2018). About 85% of stroke is caused by ischemia (Dai et al. 2013). Stroke can impair the neuron circuit and function (Han et al. 2018, Zhou et al. 2016). It disrupts not only the infarct area, but also the surrounding peri-ischemic areas (Hodges 1995). Stroke is a medical emergency, therefore, preventive and early action or other complications to reduce brain damage is crucial. However, limited drugs could protect the progression of stroke. Thus, finding new alternative therapeutic agents is required.

Buyang Huanwu Decoction (BHD) has been used for stroke in China for many years (Guo et al. 2015). Clinical trials have indicated that BHD could ameliorate the outcomes of stroke patients (Han et al. 2018, Hao et al. 2012, Zheng et al. 2018). BHD can protect against cerebral ischemia-reperfusion injury by promoting growth and differentiation of neuron (Jayakumar et al. 2015, Liu et al. 2013), inhibiting neural apoptosis and inflammation (Li et al. 2014), promoting angiogenesis and improving cerebral circulation (Zhang et al. 2016). Autophagy, a main degradation pathway, is essential for maintaining cellular homeostasis (Duan et al. 2018). Autophagy primarily exists in peri-ischemic areas when stroke happened (Liang et al. 2015). In addition, enhancement of autophagy had neuroprotective effect on cerebral ischemia (Sun et al. 2018). The proteins of sirtuin family can mediate autophagy (Chen et al. 2018). Among them, SIRT1 knockout mice indicated that SIRT1 is a critical regulator of autophagy (Tang et al. 2018). SIRT1 can regulate autophagic pathway under different conditions (Carloni et al. 2014, Wang et al. 2012b). In addition, SIRT1 may play an important role during stroke process. Whether SIRT1/autophagy pathway involved in the protective effect of BHD against stroke is still unknown.

In this study, we verified the neuroprotective effect of BHD against stroke in MCAO-R rats. In addition, we found BHD might produce neuroprotection effect on MCAO-R by regulating SIRT1/autophagy pathway in the peri-ischemic brain.

Materials And Methods

1. Animals

Male SD rats, 270–280 g, were supplied by the Experimental Animal Centre of Guangzhou University of Chinese Medicine. All rats were raised in the center of laboratory animal of Guangzhou University of Chinese Medicine, with a 12-hour light/dark schedule, and give free access to food and water. All experimental procedures were carried out according to the Guangzhou University of Chinese Medicine Administrative Panel on Laboratory Animal Care. After one week of adaptive housing and feeding, animals were divided into 6 groups (n = 10 each group) randomly, which received sham operation as control, middle cerebral artery occlusion and reperfusion operation as model, rapamycin, BHD (5, 10 and 20 g/kg), respectively.

2. Rat middle cerebral artery occlusion and reperfusion model

Transient focal cerebral ischemia model was induced by MCAO-R model, which as described previously (Su et al. 2014, Luo et al. 2017). Briefly, rats were anesthetized with 4% isoflurane and maintained with 1.5% isoflurane via Vaporizer for Isoflurane (RWD Life Science, Shenzhen, China), a midline neck incision was to expose the right common carotid artery (CCA), the external carotid artery (ECA) and the internal carotid artery (ICA). A 4 – 0 silicone rubber-coated nylon monofilament was inserted into ECA, then gently advanced into the ICA about 17–19 mm from the carotid bifurcation to occlude the origin of middle cerebral artery (MCA). After 2 h of occlusion, the monofilament was gently removed to restore blood flow.

During the whole surgery body temperature of the rats were maintained at about 37 °C. Rats were anaesthetized by sodium pentobarbital and sacrificed at the 5th day after surgery for relevant detection.

3. Drug administration

BHD was prepared according to previous studies (Liao et al. 2018, Shen et al. 2016). All ingredients were purchased from the Guangzhou Zhixin Chinese Herbal Medicine Co. Ltd. (Guangzhou, China). All groups rats were treated with intraperitoneal injection of Hydroxychloroquine (HCQ, Selleck, S4430, 20 mg/kg) at 30 min after surgery (Huang et al. 2016). BHD powder and rapamycin (Rapa, Selleck, S1039) were dissolved with 0.9% saline. At the onset of the reperfusion (Chong et al. 2010), the treatment groups, including MCAO-R + BHD and MCAO-R + Rapa were administrated with BHD (5, 10 and 20 g/kg) by gavage and Rapa (10 mg/kg) via intraperitoneal injection respectively.

4. Neurological scores

A modified Neurological Severity Score (mNSS) test was used to calculated the neurological deficit on day 5 after surgery (Xia, Zhang and Zhao 2018, Yang et al. 2018). Higher score indicates more severe behavioral deficits.

5. Measurement of cerebral infarct size

Rat brains were rapidly sliced with a rat brain matrix (RWD Life Science, Shenzhen, China). The sections were stained with 2, 3, 5-triphenyltetrazolium hydrochloride (TTC; Sigma, T8877) (Song et al. 2013). Then photographic images were taken.

6. HE and Nissl stainings

Brain paraffin sections were prepared. Then, the sections were washed in PBS and stained with HE or Nissl reaction mixture. The sections were then washed with PBS. Images were analyzed by using a light microscope (Leica Microsystems, Wetzlar, Germany).

7. Western blot analysis

The brain peri-ischemic area and the corresponding area were homogenized in RIPA buffer. Protein samples were separated by SDS-polyacrylamide gels, and then transferred to PVDF membranes. The membranes were incubated with the primary antibody (SIRT1, LC3, Beclin 1, P62, DCX, ACTB) overnight, and then incubated with HRP-conjugated second antibody for 1 h. Blots Digital images were visualized with an Image Lab (Bio-Rad).

8. Immunofluorescence

Rat brains sections were blocked with BSA. Then they were incubated overnight at 4 °C with primary antibody (Nestin, LC3, BDNF, DCX). The slices were incubated with fluorescence-coupled secondary antibody. After rinsing, sections were incubated with DAPI. We detected fluorescence with laser scanning confocal microscope (ZEISS 8.0, Germany).

9. Statistical analysis

The data analyses were performed with SPSS 17. Data are presented as mean \pm SD. One-way analysis of variance (ANOVA) and an unpaired *t*-test were used. Differences were considered as significant at $p < 0.05$.

Results

BHD Ameliorates Infarction and Reduces Neurological Scores after MCAO-R

The plan of this study was showed in Fig. 1. We firstly observed the infarct volumes of the brain. TTC staining showed that infarct volumes of in MCAO-R + BHD group were markedly decreased than those in MCAO-R group in a dose-dependent manner (Fig. 2A and B). Two BHD groups improved neurological outcomes after MCAO-R (Fig. 2C). The dosage of BHD was determined as 20 g/kg in further study. These data demonstrated that BHD could effectively ameliorate infarction and reduces neurological score after MCAO-R.

BHD Protects Against Neural Death after MCAO-R

As shown in Fig. 3A and B (HE and Nissl staining), large areas of neuronal necrosis were induced by cerebral ischemia-reperfusion. MCAO-R group exhibited massive neurons died, with disappearance of the cytoplasmic bodies, swelling of cell bodies, nuclear condensation and sparse nissl bodies (Normal neurons showed clear and large cell nucleus and bodies). BHD reversed these changes. These data demonstrated that BHD could protect against neural death after MCAO-R.

BHD Activates SIRT1 and Autophagy in Rat Cerebral Peri-ischemic Area after MCAO-R.

In order to determine whether SIRT1/autophagy pathway was involved in the protective effect of BHD, SIRT1 and autophagic markers (LC3, P62 and Beclin-1) were detected by western blot (Fig. 4A-E). Results showed that the expression of SIRT1 in MCAO-R group and MCAO-R + BHD group was elevated. MCAO-R + BHD group showed a significantly enhanced elevation of SIRT1 than in MCAO-R group. BHD promotes SIRT1 expression in cerebral ischemia-reperfusion-induced injury. Meanwhile, the expressions of LC3-II and Beclin-1 were increased, while P62 was down-regulated in rat cerebral peri-ischemic area of MCAO-R group slightly. Then post-conditioned with BHD dramatically increased the status of autophagy, when compared with MCAO-R group. Rapa treatment showed a similar effect compared with BHD group. In addition, we elucidated the distribution pattern of Nestin and LC3 by tissue immunostaining. The expression pattern of LC3 is similar to western blot analysis (Fig. 5A and B). Nestin, a protein marker for neural stem cell, was also elevated by BHD. These data suggested that the protective effect of BHD might be related with SIRT1/autophagy pathway.

BHD Improves BDNF and DCX Expressions in Rat Cerebral Peri-ischemic Area after MCAO-R.

The expressions of BDNF and DCX (a microtubule-associated protein expressed by neuronal precursor cells) were further determined by immunostaining or western blot. MCAO-R induced the downregulations of BDNF and DCX. Post-conditioned with BHD caused a significant increase in BDNF and DCX expressions in MCAO-R rats (Figs. 6 and 7). Collectively, these results supported that neuroprotective effect of BHD in MCAO-R rats.

Discussion

In this study, we found that BHD could ameliorate infarction and reduce neurological scores at the 5th day after MCAO-R in rats. BHD treatment showed the similar trends on regulating autophagy with Rapa. Furthermore, our results found that SIRT1 was up-regulated in rat cerebral peri-ischemic area. In addition, BHD treatment improves Nestin, BDNF and DCX expressions in MCAO-R rats, which supported the neuroprotective effect of BHD. Thus, our results demonstrated that BHD activated SIRT1/autophagy pathway to produce neuroprotective effect against stroke.

The lack of blood flow during stroke making complicated pathophysiological which leads to neurons damaged, such mechanisms mainly includes excitotoxicity, mitochondrial dysfunction, Calcium overload, oxidative stress, protein misfolding, inflammatory changes and neuronal apoptosis(Hossmann 2006). Nowadays, clinical treatment of stroke mainly includes intravenous injection of tissue plasminogen activator during acute period, restore blood flow of the penumbral tissue, giving neurotrophic factor to protect neurons and symptomatic treatment. However, a large number of stroke patients are unable to receive the acute treatments owing to the narrow time windows(George and Steinberg 2015). Besides, blood flow recovery in a short time usually cause more damage to the neurons(Zhang et al. 2005). Therefore, discover more neurotrophic drugs plays a crucial role to treat stroke.

MCAO has been a valuable model of stroke since 1981, which is a model that can better simulate human stroke(Lopez and Vemuganti 2018). mNSS test is a classic test used to calculate the neurological deficit in rat after MCAO-R. Higher score indicates more severe behavioral deficits. TTC staining of the brain tissue is used to describe the level of brain damage after MCAO-R in rat. BHD significantly ameliorated neurological deficit and the level of brain damage in rat after MCAO-R. After MCAO-R, neurons became cytoplasmic bodies disappeared, cell bodies swelling, nuclear condensed and nissl bodies sparse. But BHD ameliorate this condition. Thus, BHD can protect neurons against MCAO-R.

Autophagy, a dynamic process, in which a cell degraded its own substance though surrounded by a lysosome and a bilayer membrane, fluctuates constantly(Lee et al. 2010). In central nervous system, moderate autophagy activation might be a manifestation of endogenous neuroprotective mechanisms (Hou et al. 2019). LC3-I converted to LC3-II, indicating the onset of autophagy (Corona Velazquez and Jackson 2018). SQSTM1/P62 binds directly to LC3 and is then degraded by the autophagy-lysosomal pathway (Li et al. 2018, Wang et al. 2018). Beclin-1 is a specific gene involved in autophagy and always be seen as a marker of autophagy(Ashkenazi et al. 2017). In this study, BHD and Rapa significantly

increased LC3-II and Beclin-1 compared with MCAO-R group, while down-regulated P62 expression in rat cerebral peri-ischemic area. Confocal microscopy showed that LC3 isoforms were located in living post-ischemic cells. BHD increased the enhancement of rat peri-ischemic brain autophagy at the 5th day after MCAO-R.

SIRT1, a NAD + dependent deacetylase, is well-known as a modulator of aging(Lapierre et al. 2015). SIRT1 has the function of anti-inflammatory, anti-apoptotic, antioxidation, DNA repair, maintain energy metabolism, adjust autophagy when stroke happened(Zhang, Zhang and Wu 2018).SIRT1 can interact with several essential components of the autophagy (Chen et al. 2018). Besides, research has shown that SIRT1 plays a role of brain protection might through activating autophagy pathways during stroke(Wang et al. 2012a).In this study, BHD were proven to elevate SIRT1 expression, which might be the upstream of autophagy.

Nestin is expressed from neural stem cells and neural progenitor cells (Bojnordi et al. 2017, Dey et al. 2017), which might participate in neurogenesis after stroke (Su et al. 2014). And Brain-derived neurotrophic factor (BDNF), identified as one of the critical growth factors promotes the neuronal survival and regulate the different neuronal functions such as differentiation, migration and synaptic function in CNS (Song et al. 2013). DCX is used as a marker for neurogenesis (Shahsavani et al. 2018). Results of Immunofluorescence showed that the expression of Nestin, BDNF and DCX decreased significantly after MCAO-R, whereas the stimulation of BHD could greatly enhance their expressions compared with MCAO-R group, which provided the evidence that BHD played a critical role of neuroprotection.

Conclusion

Our results have provided in vivo evidences that autophagy was activated state at the 5th day after cerebral ischemia-reperfusion and post-conditioning with BHD showed the similar trends on regulating autophagy with Rapa. Furthermore, our results found that SIRT1 was up-regulated when MCAO-R happened and BHD exacerbated this phenomenon. In addition, BHD treatment improves Nestin, BDNF and DCX expressions in MCAO-R rats, which supported the neuroprotective effect of BHD. Thus, our results demonstrated that BHD activated SIRT1/autophagy pathway to produce neuroprotective effect against stroke. However, the underlying mechanisms are still need to further explore.

Abbreviations

BHD Buyang Huanwu Decoction

MCAO-R middle cerebral artery occlusion and reperfusion

mNss modified neurological severity score

BDNF brain-derived neurotrophic factor

DCX doublecortin on the X-chromosome

SIRT1 Sirtuin1

Rapa rapamycin

HE staining hematoxylin-eosin staining

LC3 Microtubule-associated protein 1 Light chain 3

SQSTM1/P62 Sequestosome1

SD Rat Sprague-Dawley Rat

CCA common carotid artery

ECA external carotid artery

ICA internal carotid artery

MCA middle cerebral artery

TTC 2, 3, 5-triphenyltetrazolium hydrochloride

PBS Phosphate Buffered Saline

SDS Sodium Dodecyl Sulfate

PVDF Polyvinylidene Fluoride

HRP Horseradish Peroxidase

BSA Bovine Serum Albumin

DAPI 4,6-diamino-2-phenyl indole

TCM Tradition Chinese Medicine

Declarations

Ethics approval and consent to participate

The Animal Ethics Committee approved experimental protocols of Guangzhou University of Chinese Medicine, and experiments were performed in compliance with relative protocols.

Consent to publish

All of authors consent to publication of this work in Chinese Medicine.

Availability of data and materials

Not applicable.

Competing interests

The authors declare that they have no competing interests.

Funding

This work was supported by the National Natural Science Foundation of China (No.81673717) and Guangdong Provincial Key Laboratory of Research on Emergency in TCM (2017B030314176).

Authors' Contributions

Han Li and Yang Zhang carried to most of the experiments and wrote the manuscript. Shi-Jie Zhang designed the experiments. Dong Peng, Hao Lin, Shi-Jie Zhang and Li Guan modified manuscript.

Acknowledgements

Not applicable.

References

- Ashkenazi, A., C. F. Bento, T. Ricketts, M. Vicinanza, F. Siddiqi, M. Pavel, F. Squitieri, M. C. Hardenberg, S. Imarisio, F. M. Menzies & D. C. Rubinsztein (2017) Polyglutamine tracts regulate beclin 1-dependent autophagy. *Nature*, 545, 108-111.
- Benjamin, E. J., S. S. Virani, C. W. Callaway, A. M. Chamberlain, A. R. Chang, S. Cheng, S. E. Chiuve, M. Cushman, F. N. Delling, R. Deo, S. D. de Ferranti, J. F. Ferguson, M. Fornage, C. Gillespie, C. R. Isasi, M. C. Jimenez, L. C. Jordan, S. E. Judd, D. Lackland, J. H. Lichtman, L. Lisabeth, S. Liu, C. T. Longenecker, P. L. Lutsey, J. S. Mackey, D. B. Matchar, K. Matsushita, M. E. Mussolino, K. Nasir, M. O'Flaherty, L. P. Palaniappan, A. Pandey, D. K. Pandey, M. J. Reeves, M. D. Ritchey, C. J. Rodriguez, G. A. Roth, W. D. Rosamond, U. K. A. Sampson, G. M. Satou, S. H. Shah, N. L. Spartano, D. L. Tirschwell, C. W. Tsao, J. H. Voeks, J. Z. Willey, J. T. Wilkins, J. H. Wu, H. M. Alger, S. S. Wong, P. Muntner, E. American Heart Association Council on, C. Prevention Statistics & S. Stroke Statistics (2018) Heart Disease and Stroke Statistics-2018 Update: A Report From the American Heart Association. *Circulation*, 137, e67-e492.
- Bojnordi, M. N., H. Azizi, T. Skutella, M. Movahedin, F. Pourabdolhossein, A. Shojaei & H. G. Hamidabadi (2017) Differentiation of Spermatogonia Stem Cells into Functional Mature Neurons Characterized with Differential Gene Expression. *Mol Neurobiol*, 54, 5676-5682.
- Carloni, S., M. C. Albertini, L. Galluzzi, G. Buonocore, F. Proietti & W. Balduini (2014) Melatonin reduces endoplasmic reticulum stress and preserves sirtuin 1 expression in neuronal cells of newborn rats after

hypoxia-ischemia. *J Pineal Res*, 57, 192-9.

Chen, X., Z. Pan, Z. Fang, W. Lin, S. Wu, F. Yang, Y. Li, H. Fu, H. Gao & S. Li (2018) Omega-3 polyunsaturated fatty acid attenuates traumatic brain injury-induced neuronal apoptosis by inducing autophagy through the upregulation of SIRT1-mediated deacetylation of Beclin-1. *J Neuroinflammation*, 15, 018-1345.

Chong, Z. Z., Y. C. Shang, L. Zhang, S. Wang & K. Maiese (2010) Mammalian target of rapamycin: hitting the bull's-eye for neurological disorders. *Oxid Med Cell Longev*, 3, 374-91.

Corona Velazquez, A. F. & W. T. Jackson (2018) So Many Roads: the Multifaceted Regulation of Autophagy Induction. *Mol Cell Biol*, 38, 00303-18.

Dai, W., X. Liu, Z. Zhang, J. Chen, R. Guo, H. Zheng, X. Jin, S. Wen, Y. Gao, T. Li, P. Lu & Y. Zhang (2013) A two-level model for the analysis of syndrome of acute ischemic stroke: from diagnostic model to molecular mechanism. *Evid Based Complement Alternat Med*, 293010, 4.

Dey, A., P. Farzanehfar, E. V. Gazina & T. D. Aumann (2017) Electrophysiological and gene expression characterization of the ontogeny of nestin-expressing cells in the adult mouse midbrain. *Stem Cell Res*, 23, 143-153.

Duan, X., B. Chen, Y. Cui, L. Zhou, C. Wu, Z. Yang, Y. Wen, X. Miao, Q. Li, L. Xiong & J. He (2018) Ready player one? Autophagy shapes resistance to photodynamic therapy in cancers. *Apoptosis*, 23, 587-606.

Feigin, V. L., G. Nguyen, K. Cercy, C. O. Johnson, T. Alam, P. G. Parmar, A. A. Abajobir, K. H. Abate, F. Abd-Allah, A. N. Abejie, G. Y. Abyu, Z. Ademi, G. Agarwal, M. B. Ahmed, R. O. Akinyemi, R. Al-Raddadi, L. N. Aminde, C. Amlie-Lefond, H. Ansari, H. Asayesh, S. W. Asgedom, T. M. Atey, H. T. Ayele, M. Banach, A. Banerjee, A. Barac, S. L. Barker-Collo, T. Bärnighausen, L. Barregard, S. Basu, N. Bedi, M. Behzadifar, Y. Béjot, D. A. Bennett, I. M. Bensenor, D. F. Berhe, D. J. Boneya, M. Brainin, I. R. Campos-Nonato, V. Caso, C. A. Castañeda-Orjuela, J. C. Rivas, F. Catalá-López, H. Christensen, M. H. Criqui, A. Damasceno, L. Dandona, R. Dandona, K. Davletov, B. de Courten, G. deVeber, K. Dokova, D. Edessa, M. Endres, E. J. A. Faraon, M. S. Farvid, F. Fischer, K. Foreman, M. H. Forouzanfar, S. L. Gall, T. T. Gebrehiwot, J. M. Geleijnse, R. F. Gillum, M. Giroud, A. C. Goulart, R. Gupta, V. Hachinski, R. R. Hamadeh, G. J. Hankey, H. A. Hareri, R. Havmoeller, S. I. Hay, M. I. Hegazy, D. T. Hibstu, S. L. James, P. Jeemon, D. John, J. B. Jonas, J. Józwiak, R. Kalani, A. Kandel, A. Kasaeian, A. P. Kengne, Y. S. Khader, A. R. Khan, Y. H. Khang, J. Khubchandani, D. Kim, Y. J. Kim, M. Kivimaki, Y. Kokubo, D. Kolte, J. A. Kopec, S. Kosen, M. Kravchenko, R. Krishnamurthi, G. A. Kumar, A. Lafranconi, P. M. Lavados, Y. Legesse, et al. (2018) Global, Regional, and Country-Specific Lifetime Risks of Stroke, 1990 and 2016. *N Engl J Med*, 379, 2429-2437.

George, P. M. & G. K. Steinberg (2015) Novel Stroke Therapeutics: Unraveling Stroke Pathophysiology and Its Impact on Clinical Treatments. *Neuron*, 87, 297-309.

- Guo, Q., M. Zhong, H. Xu, X. Mao, Y. Zhang & N. Lin (2015) A Systems Biology Perspective on the Molecular Mechanisms Underlying the Therapeutic Effects of Buyang Huanwu Decoction on Ischemic Stroke. *Rejuvenation Res*, 18, 313-25.
- Han, C. H., M. Kim, S. Y. Cho, W. S. Jung, S. K. Moon, J. M. Park, C. N. Ko, K. H. Cho & S. Kwon (2018) Adjunctive herbal medicine treatment for patients with acute ischemic stroke: A systematic review and meta-analysis. *Complement Ther Clin Pract*, 33, 124-137.
- Hao, C. Z., F. Wu, J. Shen, L. Lu, D. L. Fu, W. J. Liao & G. Q. Zheng (2012) Clinical efficacy and safety of buyang huanwu decoction for acute ischemic stroke: a systematic review and meta-analysis of 19 randomized controlled trials. *Evid Based Complement Alternat Med*, 630124, 21.
- Hodges, H. (1995) Graft-induced recovery of cognitive function after diffuse and focal brain damage: implications for neural transplantation in man. *Zh Vyssh Nerv Deiat Im I P Pavlova*, 45, 29-58.
- Hossmann, K. A. (2006) Pathophysiology and therapy of experimental stroke. *Cell Mol Neurobiol*, 26, 1057-83.
- Hou, K., D. Xu, F. Li, S. Chen & Y. Li (2019) The progress of neuronal autophagy in cerebral ischemia stroke: Mechanisms, roles and research methods. *J Neurol Sci*, 400, 72-82.
- Huang, Y. T., Y. Y. Chen, Y. H. Lai, C. C. Cheng, T. C. Lin, Y. S. Su, C. H. Liu & P. C. Lai (2016) Resveratrol alleviates the cytotoxicity induced by the radiocontrast agent, ioxitalamate, by reducing the production of reactive oxygen species in HK-2 human renal proximal tubule epithelial cells in vitro. *Int J Mol Med*, 37, 83-91.
- Jayakumar, T., A. R. Elizebeth, T. L. Yen & J. R. Sheu (2015) Chinese medicines and bioactive compounds for treatment of stroke. *Chin J Integr Med*, 21, 90-101.
- Lapierre, L. R., C. Kumsta, M. Sandri, A. Ballabio & M. Hansen (2015) Transcriptional and epigenetic regulation of autophagy in aging. *Autophagy*, 11, 867-80.
- Lee, J. H., W. H. Yu, A. Kumar, S. Lee, P. S. Mohan, C. M. Peterhoff, D. M. Wolfe, M. Martinez-Vicente, A. C. Massey, G. Sovak, Y. Uchiyama, D. Westaway, A. M. Cuervo & R. A. Nixon (2010) Lysosomal proteolysis and autophagy require presenilin 1 and are disrupted by Alzheimer-related PS1 mutations. *Cell*, 141, 1146-58.
- Li, J. H., A. J. Liu, H. Q. Li, Y. Wang, H. C. Shang & G. Q. Zheng (2014) Buyang huanwu decoction for healthcare: evidence-based theoretical interpretations of treating different diseases with the same method and target of vascularity. *Evid Based Complement Alternat Med*, 506783, 14.
- Li, L., L. Jing, J. Wang, W. Xu, X. Gong, Y. Zhao, Y. Ma, X. Yao & X. Sun (2018) Autophagic flux is essential for the downregulation of D-dopachrome tautomerase by atractylenolide I to ameliorate intestinal adenoma formation. *J Cell Commun Signal*, 12, 689-698.

- Liang, K., L. Zhu, J. Tan, W. Shi, Q. He & B. Yu (2015) Identification of autophagy signaling network that contributes to stroke in the ischemic rodent brain via gene expression. *Neurosci Bull*, 31, 480-90.
- Liao, F., Y. Meng, H. Zheng, D. He, X. Shen, J. Yu, Y. Wu & L. Wang (2018) Biospecific isolation and characterization of angiogenesis-promoting ingredients in Buyang Huanwu decoction using affinity chromatography on rat brain microvascular endothelial cells combined with solid-phase extraction, and HPLC-MS/MS. *Talanta*, 179, 490-500.
- Liu, B., G. Cai, J. Yi & X. Chen (2013) Buyang Huanwu Decoction regulates neural stem cell behavior in ischemic brain. *Neural Regen Res*, 8, 2336-42.
- Lopez, M. S. & R. Vemuganti (2018) Modeling Transient Focal Ischemic Stroke in Rodents by Intraluminal Filament Method of Middle Cerebral Artery Occlusion. *Methods Mol Biol*, 1717, 101-113.
- Luo, C., M. W. Ouyang, Y. Y. Fang, S. J. Li, Q. Zhou, J. Fan, Z. S. Qin & T. Tao (2017) Dexmedetomidine Protects Mouse Brain from Ischemia-Reperfusion Injury via Inhibiting Neuronal Autophagy through Up-Regulating HIF-1 α . *Front Cell Neurosci*, 11.
- Shahsavani, M., R. J. Pronk, R. Falk, M. Lam, M. Moslem, S. B. Linker, J. Salma, K. Day, J. Schuster, B. M. Anderlid, N. Dahl, F. H. Gage & A. Falk (2018) An in vitro model of lissencephaly: expanding the role of DCX during neurogenesis. *Mol Psychiatry*, 23, 1674-1684.
- Shen, J., Y. Zhu, K. Huang, H. Jiang, C. Shi, X. Xiong, R. Zhan & J. Pan (2016) Buyang Huanwu Decoction attenuates H₂O₂-induced apoptosis by inhibiting reactive oxygen species-mediated mitochondrial dysfunction pathway in human umbilical vein endothelial cells. *BMC Complement Altern Med*, 16, 016-1152.
- Song, M., O. Mohamad, X. Gu, L. Wei & S. P. Yu (2013) Restoration of intracortical and thalamocortical circuits after transplantation of bone marrow mesenchymal stem cells into the ischemic brain of mice. *Cell Transplant*, 22, 2001-15.
- Su, J., T. Zhang, K. Wang, T. Zhu & X. Li (2014) Autophagy activation contributes to the neuroprotection of remote ischemic preconditioning against focal cerebral ischemia in rats. *Neurochem Res*, 39, 2068-77.
- Sun, Y., T. Zhang, Y. Zhang, J. Li, L. Jin, N. Shi, K. Liu & X. Sun (2018) Ischemic Postconditioning Alleviates Cerebral Ischemia-Reperfusion Injury Through Activating Autophagy During Early Reperfusion in Rats. *Neurochem Res*, 43, 1826-1840.
- Tang, Q., Q. Len, Z. Liu & W. Wang (2018) Overexpression of miR-22 attenuates oxidative stress injury in diabetic cardiomyopathy via Sirt 1. *Cardiovasc Ther*, 36, 1755-5922.
- Wang, B., C. Hu, Y. Mei, J. Bao, S. Ding, X. Liu, Q. Mei & J. Xu (2018) Resolvin D1 Resolve Inflammation in Experimental Acute Pancreatitis by Restoring Autophagic Flux. *Dig Dis Sci*, 63, 3359-3366.

- Wang, P., Y. F. Guan, H. Du, Q. W. Zhai, D. F. Su & C. Y. Miao (2012a) Induction of autophagy contributes to the neuroprotection of nicotinamide phosphoribosyltransferase in cerebral ischemia. *Autophagy*, 8, 77-87.
- Wang, Q., M. Liu, W. W. Liu, W. B. Hao, S. Tashiro, S. Onodera & T. Ikejima (2012b) In vivo recovery effect of silibinin treatment on streptozotocin-induced diabetic mice is associated with the modulations of Sirt-1 expression and autophagy in pancreatic β -cell. *J Asian Nat Prod Res*, 14, 413-23.
- Xia, D., Z. Zhang & Y. Zhao (2018) Acteoside Attenuates Oxidative Stress and Neuronal Apoptosis in Rats with Focal Cerebral Ischemia-Reperfusion Injury. *Biol Pharm Bull*, 41, 1645-1651.
- Yang, J., H. Yan, S. Li & M. Zhang (2018) Berberine Ameliorates MCAO Induced Cerebral Ischemia/Reperfusion Injury via Activation of the BDNF-TrkB-PI3K/Akt Signaling Pathway. *Neurochem Res*, 43, 702-710.
- Zhang, J. F., Y. L. Zhang & Y. C. Wu (2018) The Role of Sirt1 in Ischemic Stroke: Pathogenesis and Therapeutic Strategies. *Front Neurosci*, 12, 833.
- Zhang, S., J. Boyd, K. Delaney & T. H. Murphy (2005) Rapid reversible changes in dendritic spine structure in vivo gated by the degree of ischemia. *J Neurosci*, 25, 5333-8.
- Zhang, Z. Q., J. Y. Song, Y. Q. Jia & Y. K. Zhang (2016) Buyanghuanwu decoction promotes angiogenesis after cerebral ischemia/reperfusion injury: mechanisms of brain tissue repair. *Neural Regen Res*, 11, 435-40.
- Zheng, X. W., C. S. Shan, Q. Q. Xu, Y. Wang, Y. H. Shi & G. Q. Zheng (2018) Buyang Huanwu Decoction Targets SIRT1/VEGF Pathway to Promote Angiogenesis After Cerebral Ischemia/Reperfusion Injury. *Front Neurosci*, 12.
- Zhou, M., H. Wang, J. Zhu, W. Chen, L. Wang, S. Liu, Y. Li, L. Wang, Y. Liu, P. Yin, J. Liu, S. Yu, F. Tan, R. M. Barber, M. M. Coates, D. Dicker, M. Fraser, D. González-Medina, H. Hamavid, Y. Hao, G. Hu, G. Jiang, H. Kan, A. D. Lopez, M. R. Phillips, J. She, T. Vos, X. Wan, G. Xu, L. L. Yan, C. Yu, Y. Zhao, Y. Zheng, X. Zou, M. Naghavi, Y. Wang, C. J. L. Murray, G. Yang & X. Liang (2016) Cause-specific mortality for 240 causes in China during 1990–2013: a systematic subnational analysis for the Global Burden of Disease Study 2013. *The Lancet*, 387, 251-272.

Figures

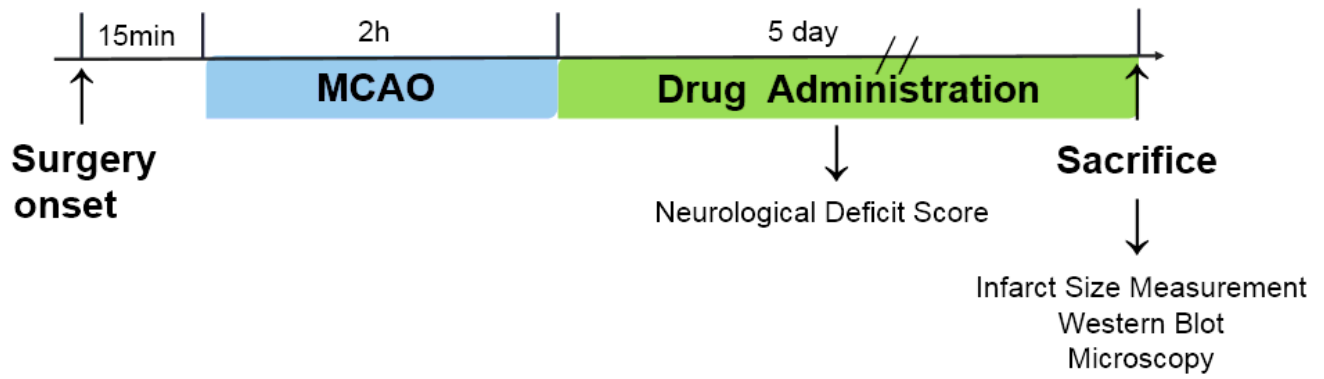


Figure 1

The schematic protocol of surgery for cerebral ischemia-reperfusion.

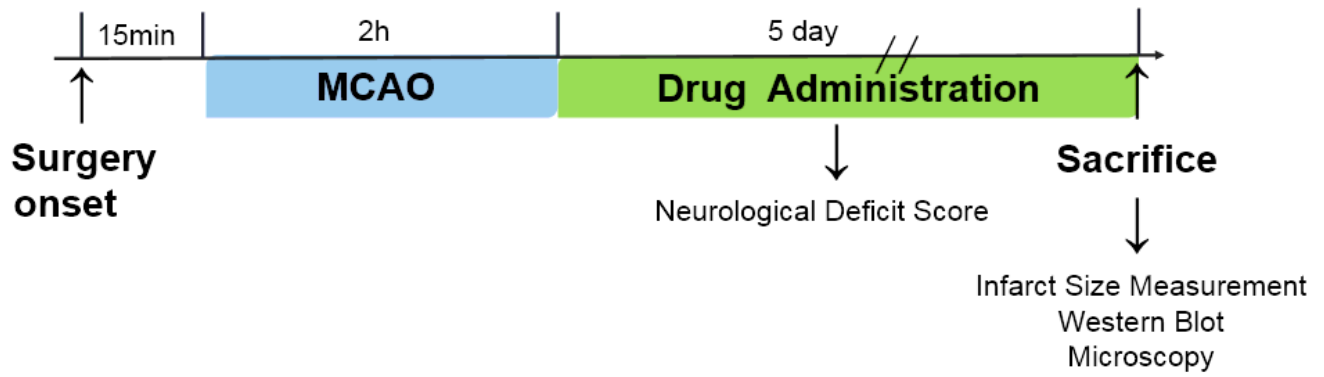


Figure 1

The schematic protocol of surgery for cerebral ischemia-reperfusion.

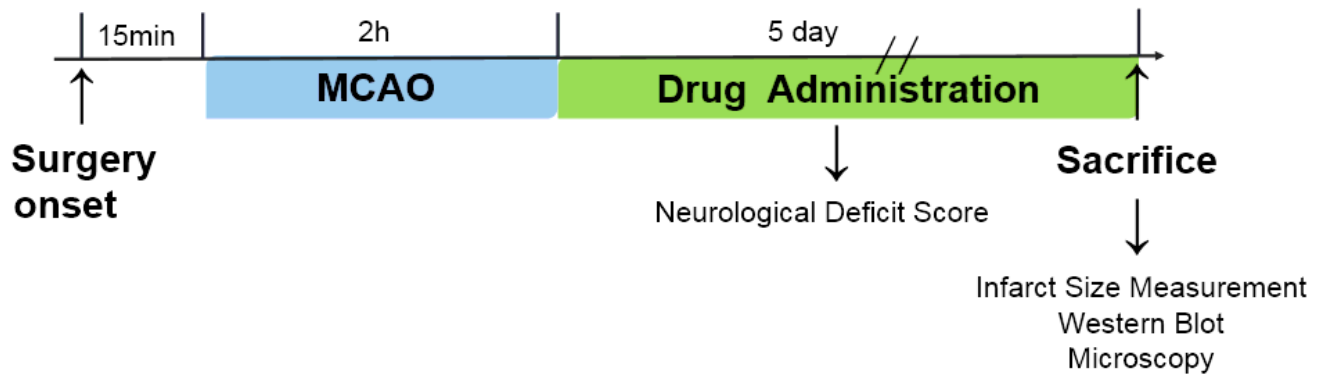


Figure 1

The schematic protocol of surgery for cerebral ischemia-reperfusion.

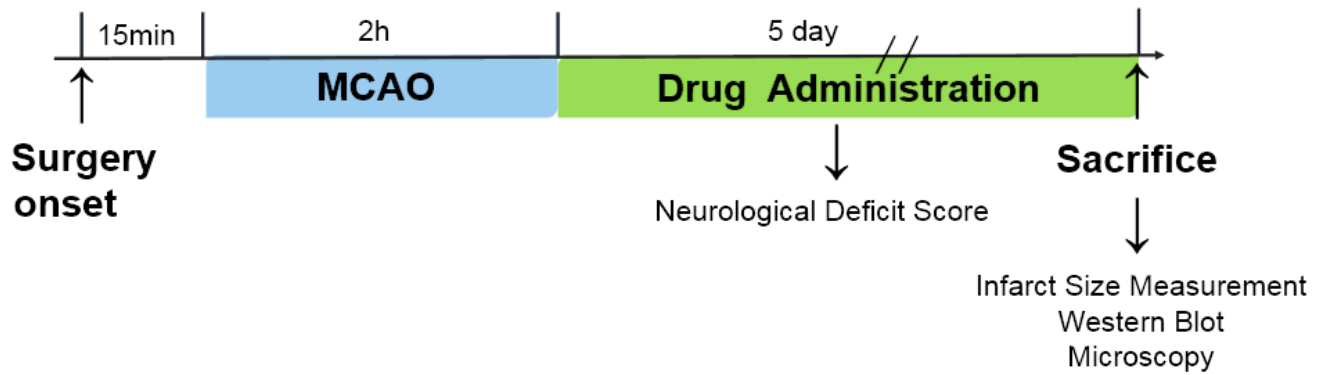
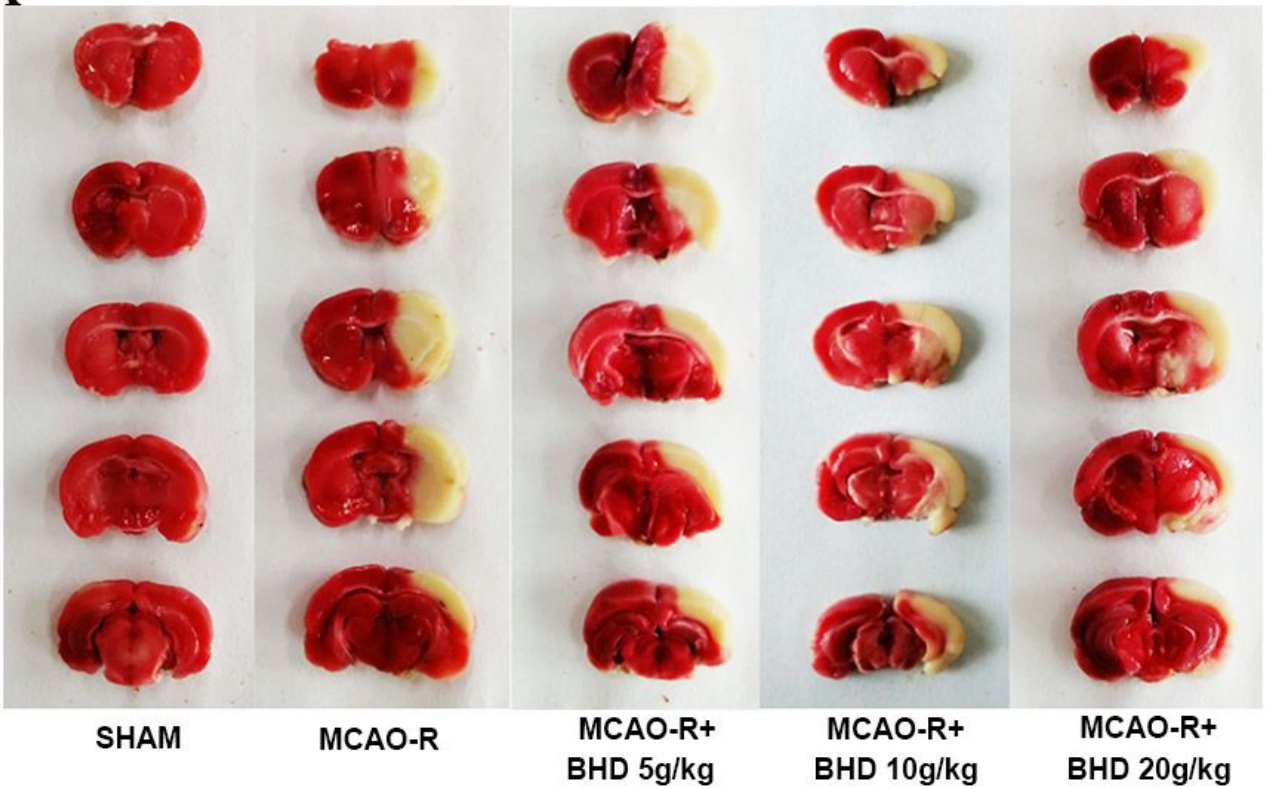
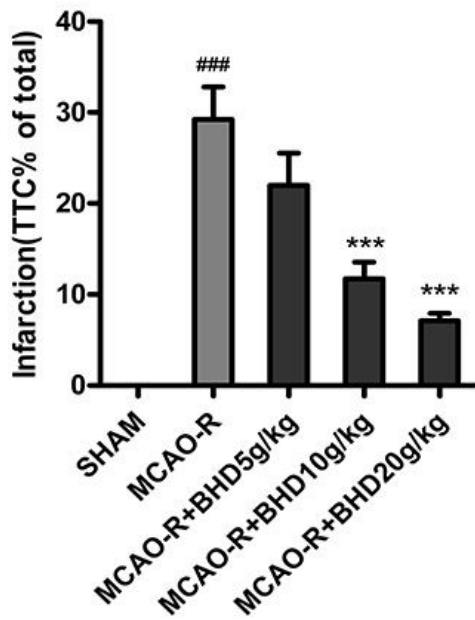
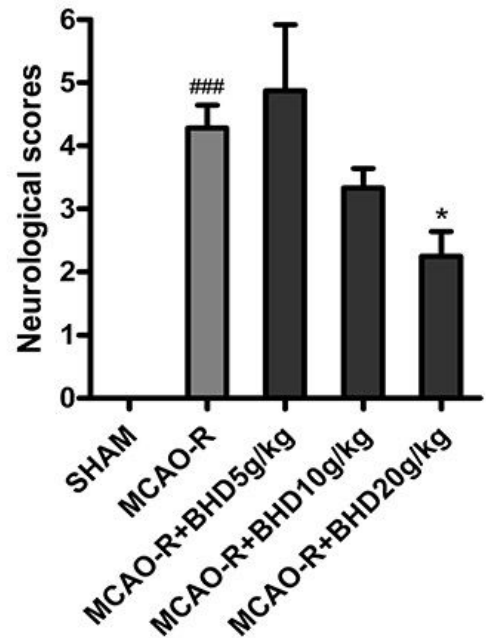
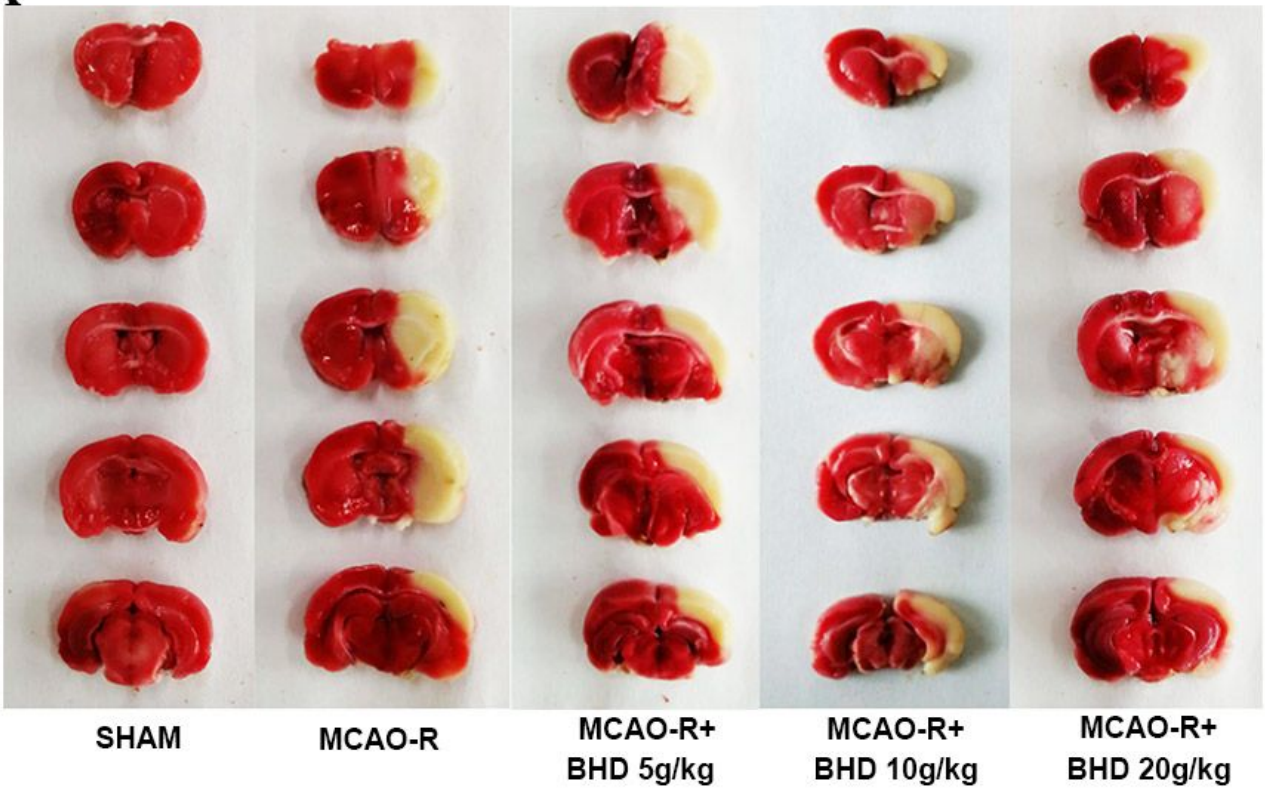
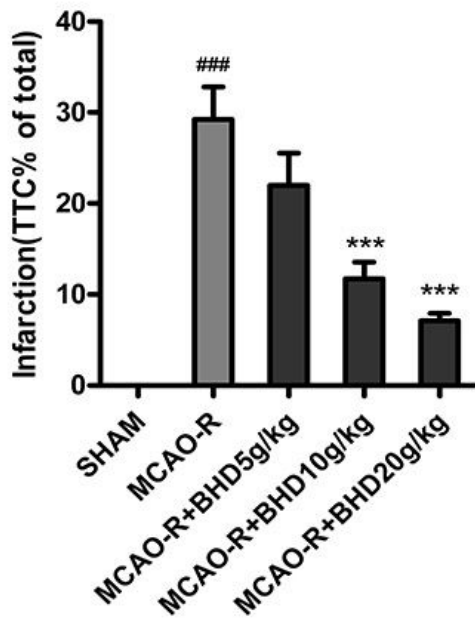
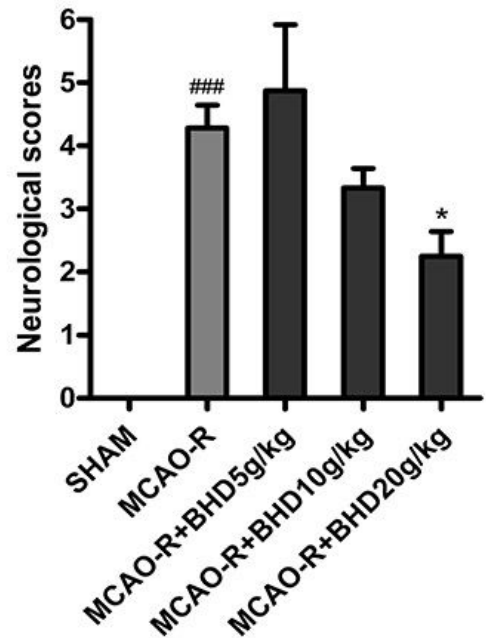


Figure 1

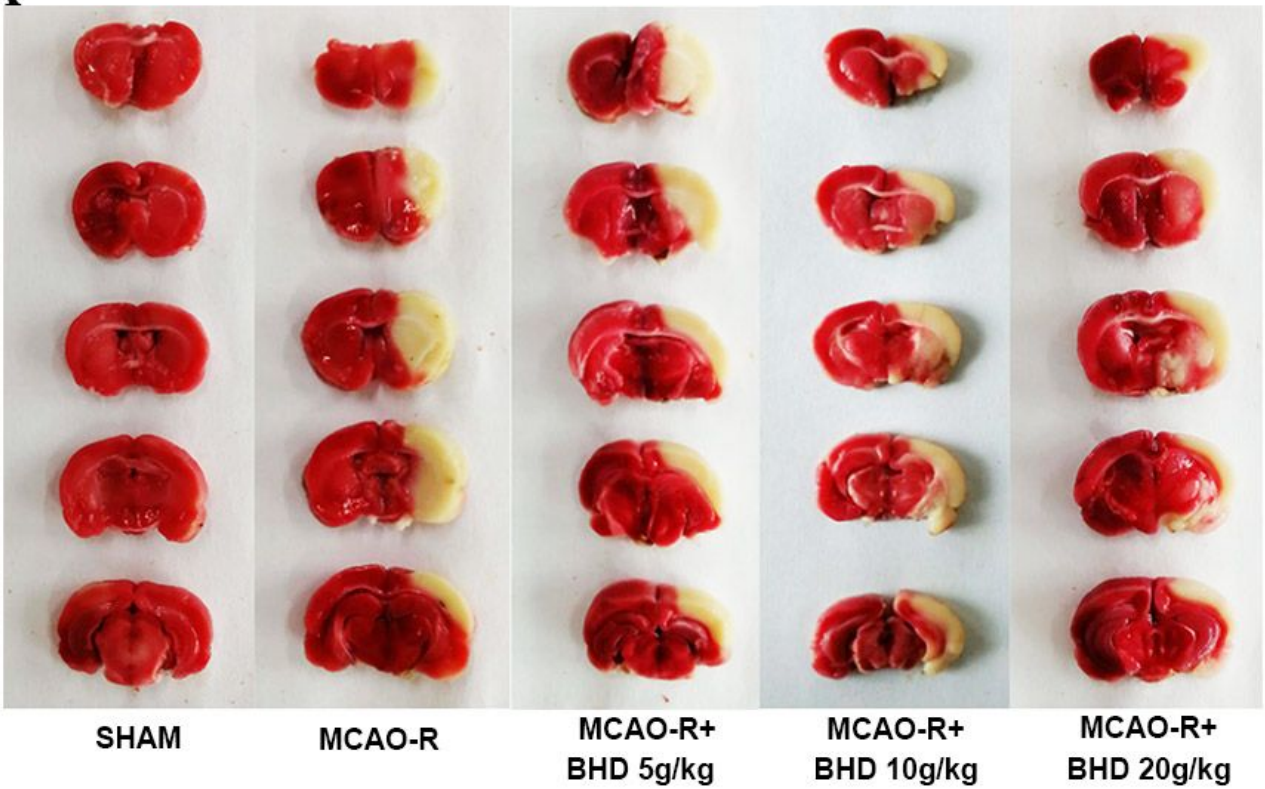
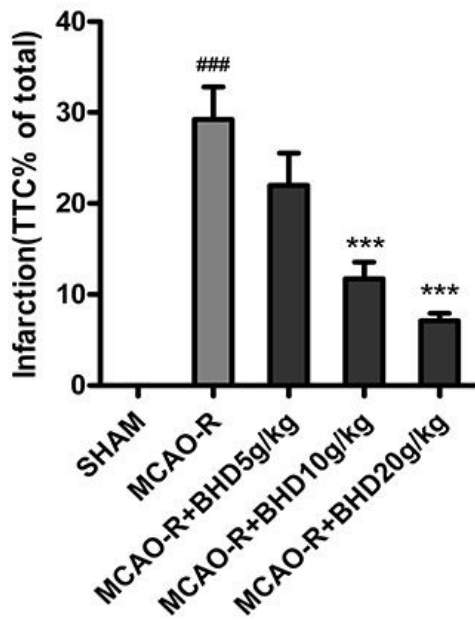
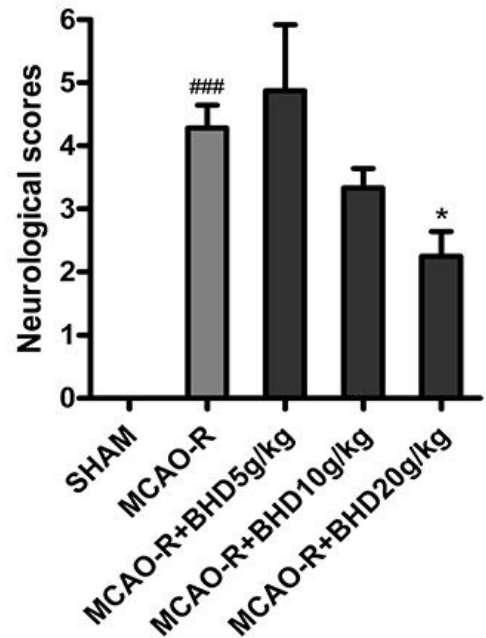
The schematic protocol of surgery for cerebral ischemia-reperfusion.

A**B****C****Figure 2**

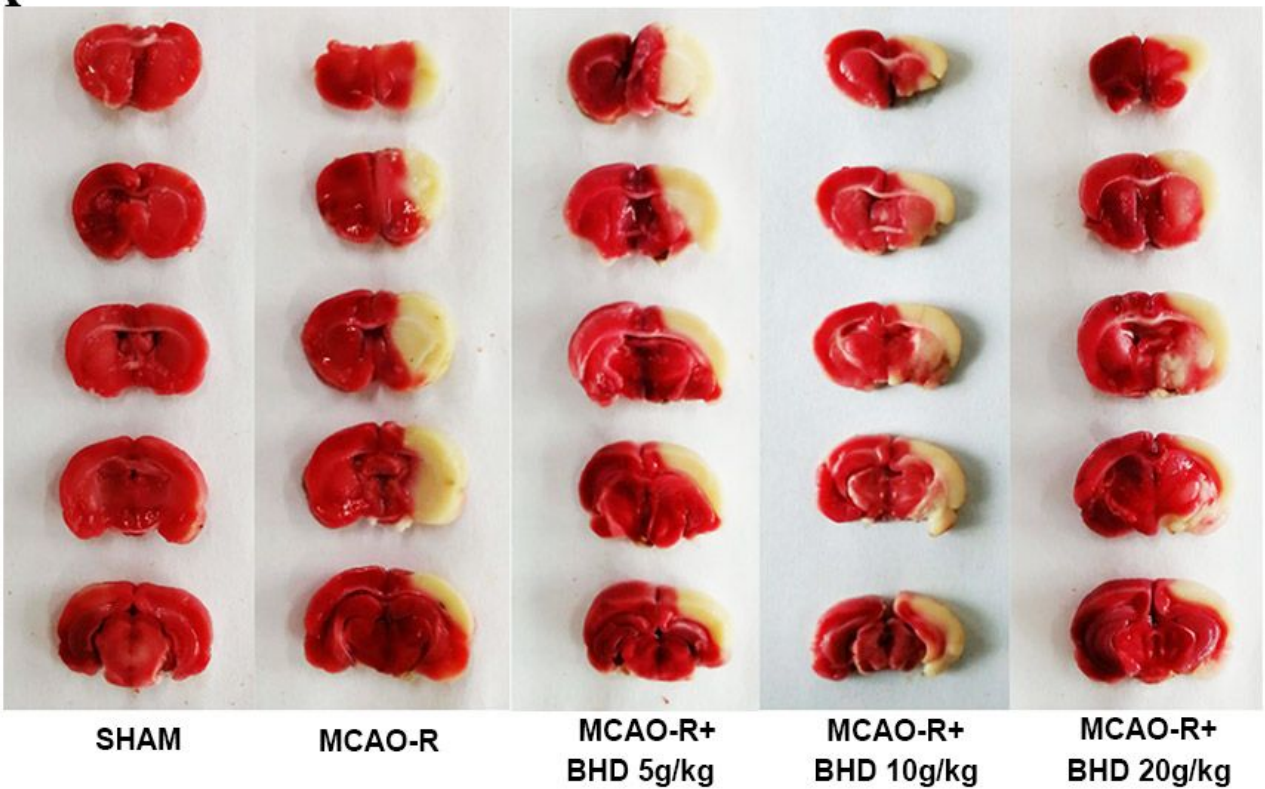
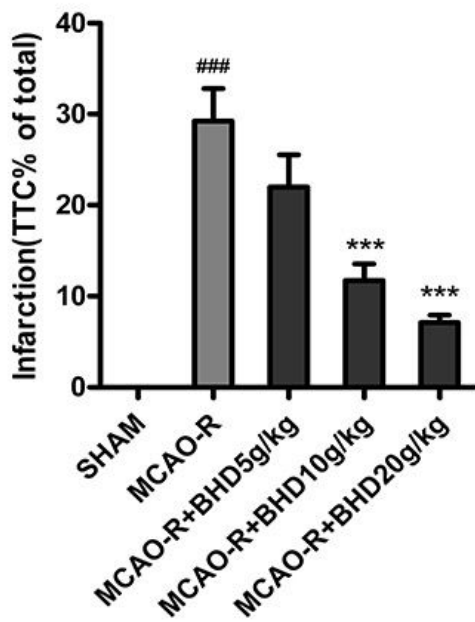
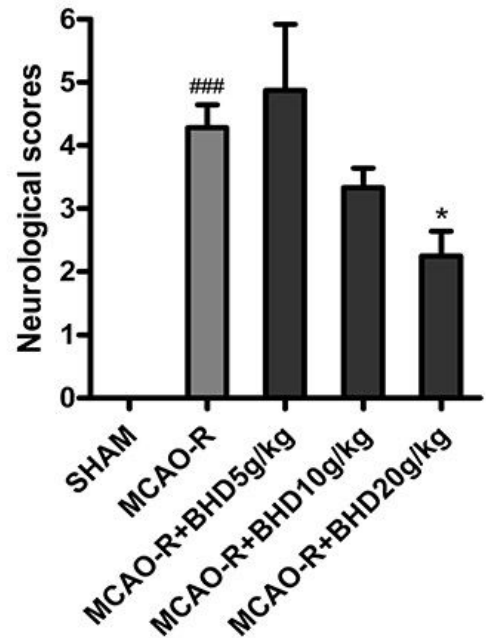
BHD alleviates ischemic brain injury. (A) Rats were subjected to 2 h of MCAO-R followed by reperfusion. The cerebral infarct volumes were determined by TTC staining. Representative TTC-stained brain slices from each group were shown. (B and C) The infarct volumes and neurological deficit scores of each group were determined. The data were expressed as means \pm SD (n = 10). Statistical comparisons were performed with one-way ANOVA followed by Dunnett's t test. #p < 0.05, ##p < 0.01, ###p < 0.001 vs. SHAM group; *p < 0.05, **p < 0.01, ***p < 0.001 vs. MCAO-R group.

A**B****C****Figure 2**

BHD alleviates ischemic brain injury. (A) Rats were subjected to 2 h of MCAO-R followed by reperfusion. The cerebral infarct volumes were determined by TTC staining. Representative TTC-stained brain slices from each group were shown. (B and C) The infarct volumes and neurological deficit scores of each group were determined. The data were expressed as means \pm SD (n = 10). Statistical comparisons were performed with one-way ANOVA followed by Dunnett's t test. #p < 0.05, ##p < 0.01, ###p < 0.001 vs. SHAM group; *p < 0.05, **p < 0.01, ***p < 0.001 vs. MCAO-R group.

A**B****C****Figure 2**

BHD alleviates ischemic brain injury. (A) Rats were subjected to 2 h of MCAO-R followed by reperfusion. The cerebral infarct volumes were determined by TTC staining. Representative TTC-stained brain slices from each group were shown. (B and C) The infarct volumes and neurological deficit scores of each group were determined. The data were expressed as means \pm SD (n = 10). Statistical comparisons were performed with one-way ANOVA followed by Dunnett's t test. #p < 0.05, ##p < 0.01, ###p < 0.001 vs. SHAM group; *p < 0.05, **p < 0.01, ***p < 0.001 vs. MCAO-R group.

A**B****C****Figure 2**

BHD alleviates ischemic brain injury. (A) Rats were subjected to 2 h of MCAO-R followed by reperfusion. The cerebral infarct volumes were determined by TTC staining. Representative TTC-stained brain slices from each group were shown. (B and C) The infarct volumes and neurological deficit scores of each group were determined. The data were expressed as means \pm SD (n = 10). Statistical comparisons were performed with one-way ANOVA followed by Dunnett's t test. #p < 0.05, ##p < 0.01, ###p < 0.001 vs. SHAM group; *p < 0.05, **p < 0.01, ***p < 0.001 vs. MCAO-R group.

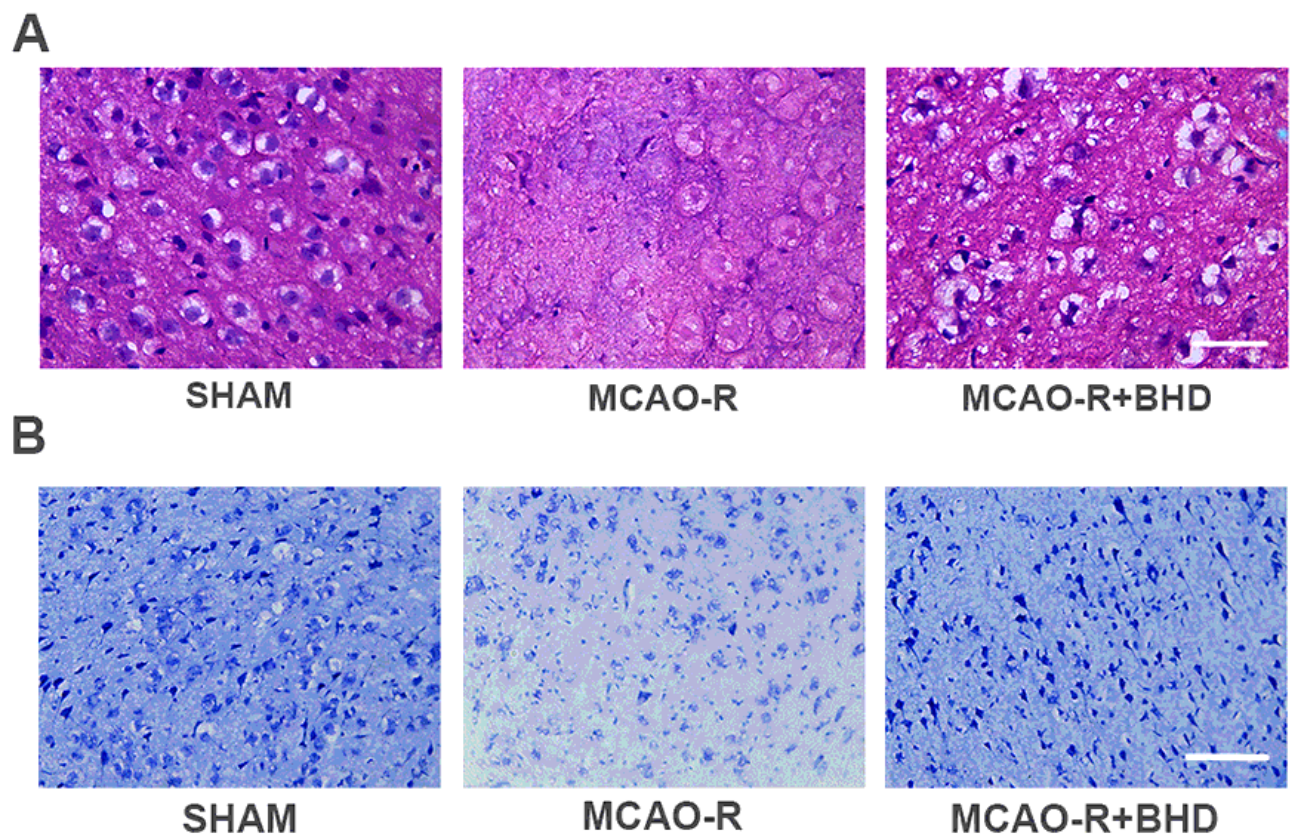


Figure 3

BHD improves the morphological alterations after MCAO-R. (A) Hematoxylin and eosin (HE) staining of the ischemic penumbra. Scale bar: 50 μ m. (Normal neurons showed clear and large cell nucleus and bodies. Damaged neurons showed disappearance of the cytoplasmic bodies, swelling of cell bodies and nuclear condensation). (B) Nissl staining of the ischemic penumbra. Scale bar: 100 μ m. (Nissl body of normal neurons showed clear and large cell bodies, Damaged neurons showed condensed nuclear and sparse Nissl bodies.)

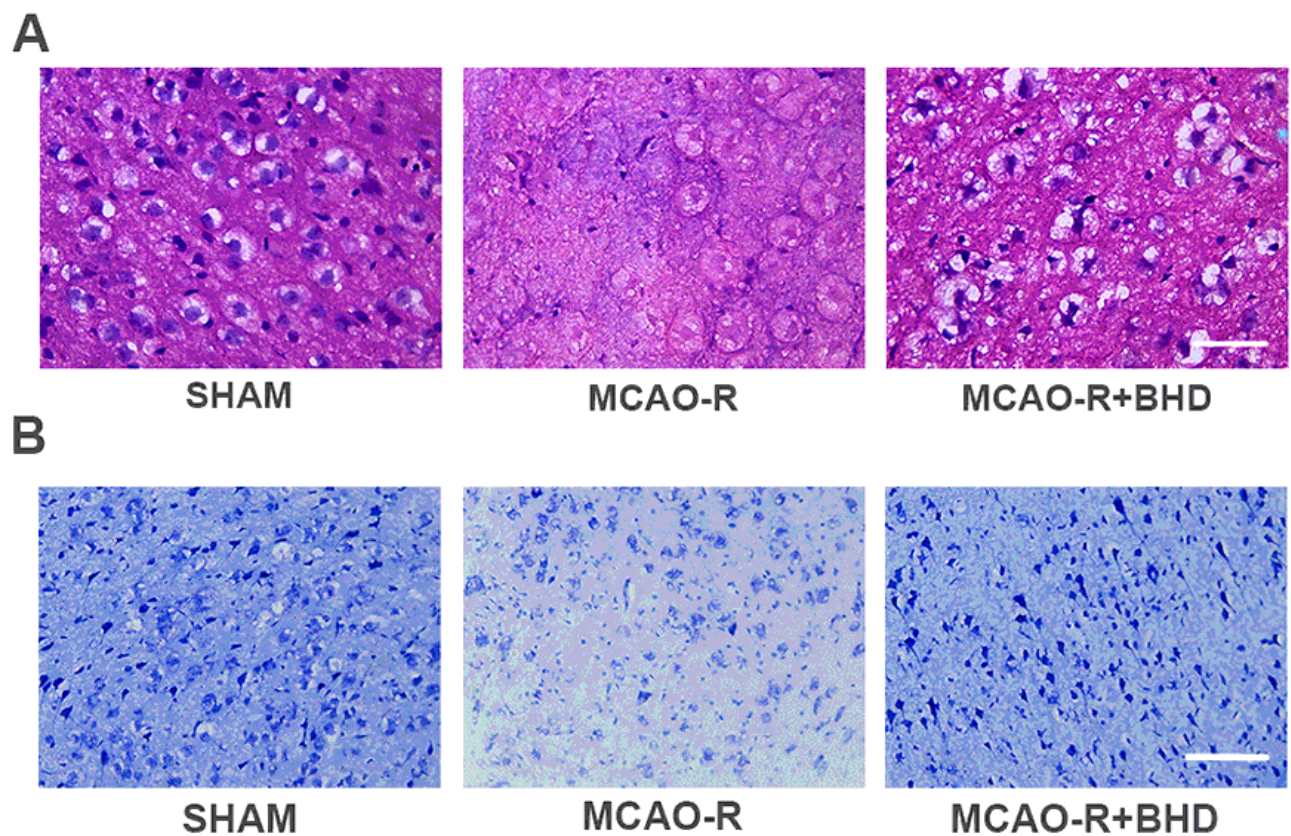


Figure 3

BHD improves the morphological alterations after MCAO-R. (A) Hematoxylin and eosin (HE) staining of the ischemic penumbra. Scale bar: 50 μ m. (Normal neurons showed clear and large cell nucleus and bodies. Damaged neurons showed disappearance of the cytoplasmic bodies, swelling of cell bodies and nuclear condensation). (B) Nissl staining of the ischemic penumbra. Scale bar: 100 μ m. (Nissl body of normal neurons showed clear and large cell bodies, Damaged neurons showed condensed nuclear and sparse Nissl bodies.)

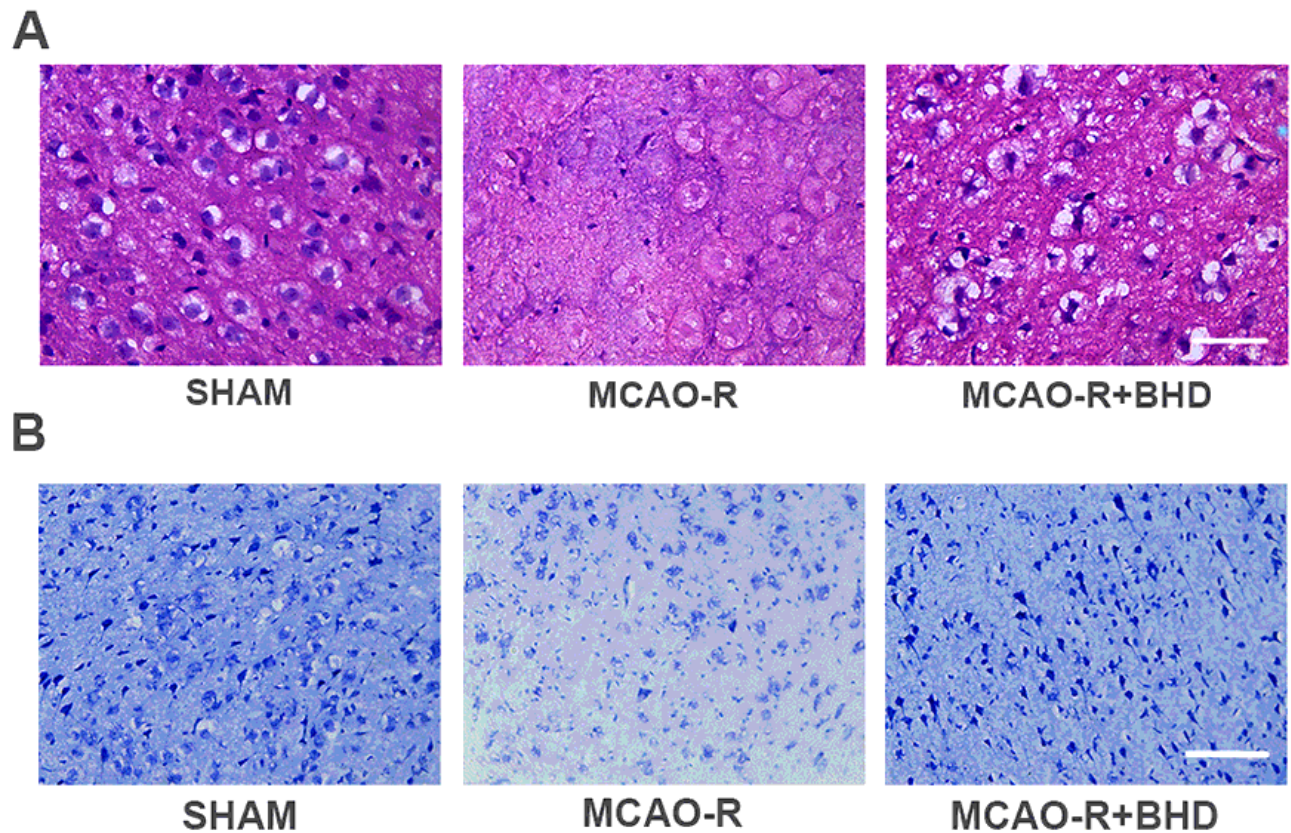


Figure 3

BHD improves the morphological alterations after MCAO-R. (A) Hematoxylin and eosin (HE) staining of the ischemic penumbra. Scale bar: 50 μ m. (Normal neurons showed clear and large cell nucleus and bodies. Damaged neurons showed disappearance of the cytoplasmic bodies, swelling of cell bodies and nuclear condensation). (B) Nissl staining of the ischemic penumbra. Scale bar: 100 μ m. (Nissl body of normal neurons showed clear and large cell bodies, Damaged neurons showed condensed nuclear and sparse Nissl bodies.)

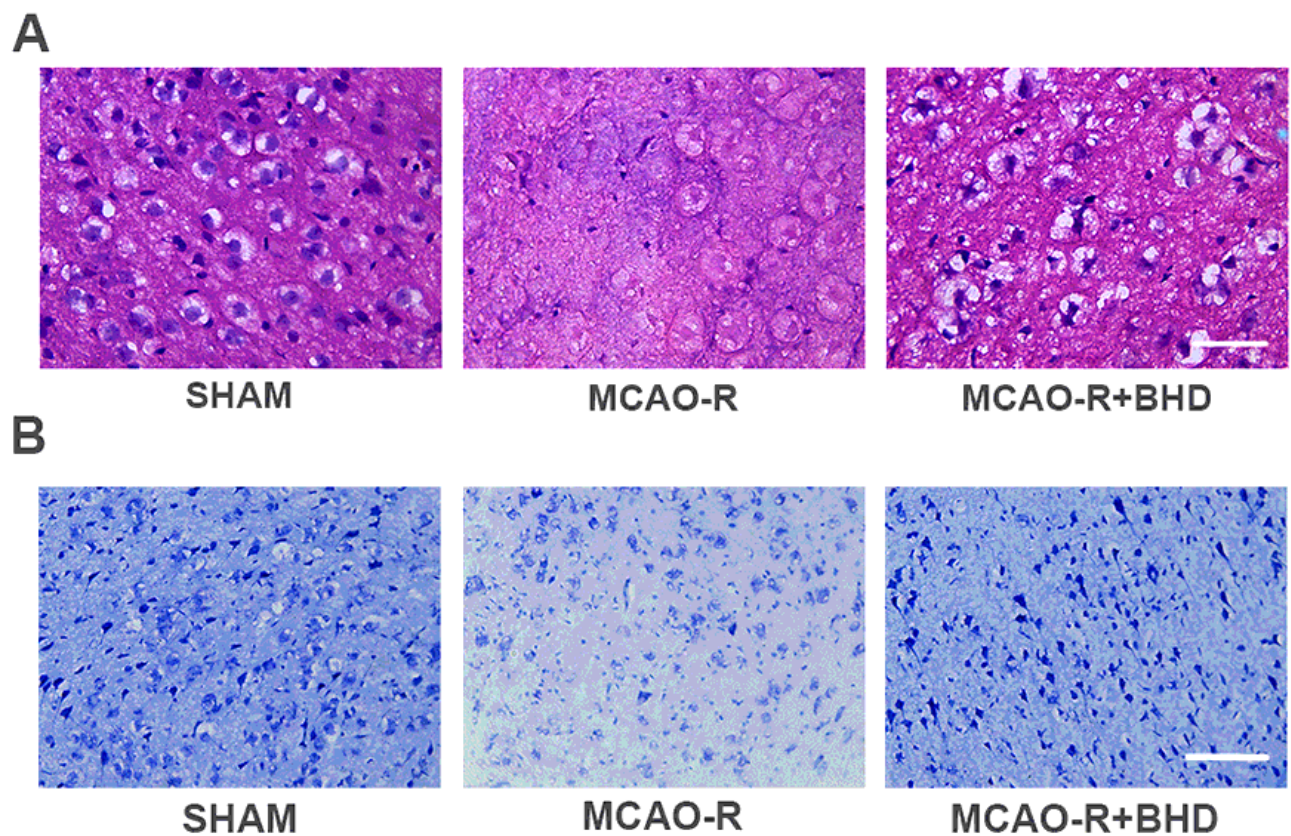


Figure 3

BHD improves the morphological alterations after MCAO-R. (A) Hematoxylin and eosin (HE) staining of the ischemic penumbra. Scale bar: 50 μ m. (Normal neurons showed clear and large cell nucleus and bodies. Damaged neurons showed disappearance of the cytoplasmic bodies, swelling of cell bodies and nuclear condensation). (B) Nissl staining of the ischemic penumbra. Scale bar: 100 μ m. (Nissl body of normal neurons showed clear and large cell bodies, Damaged neurons showed condensed nuclear and sparse Nissl bodies.)

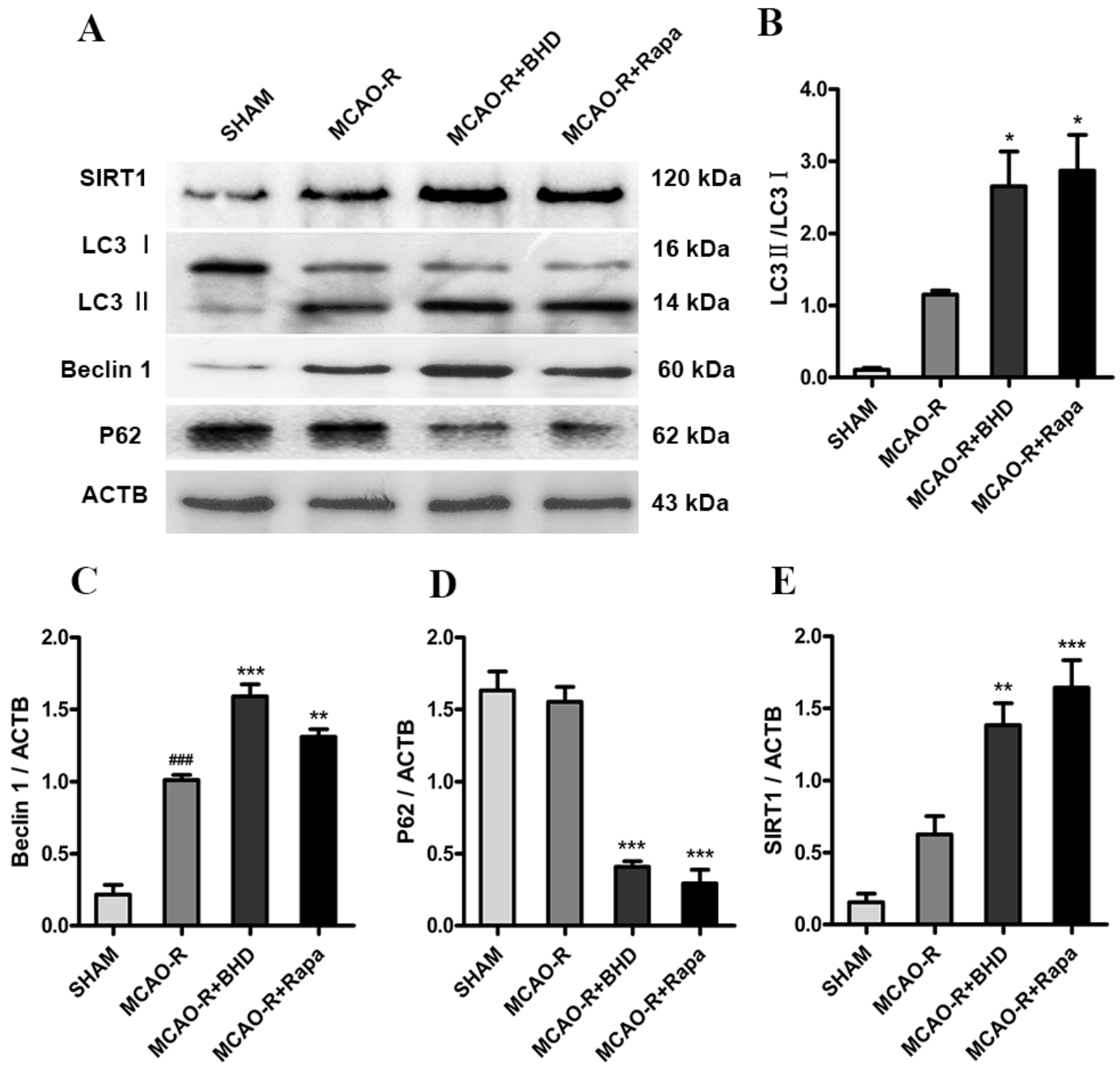


Figure 4

BHD activates SIRT1/autophagy of rat cerebral peri-ischemic area after MCAO-R. (A) Western blots of LC3, Beclin1, P62, SIRT1 in BHD-treated MCAO-R rats. (B-E) Quantitative analysis of the immunoblotted proteins was performed with Image J. Statistical comparisons were carried out with ANOVA followed by Tukey's test. Data are presented as means \pm SD (n = 3). #p < 0.05, ##p < 0.01, ###p < 0.001 vs. SHAM group; *p < 0.05, **p < 0.01, ***p < 0.001 vs. MCAO-R group.

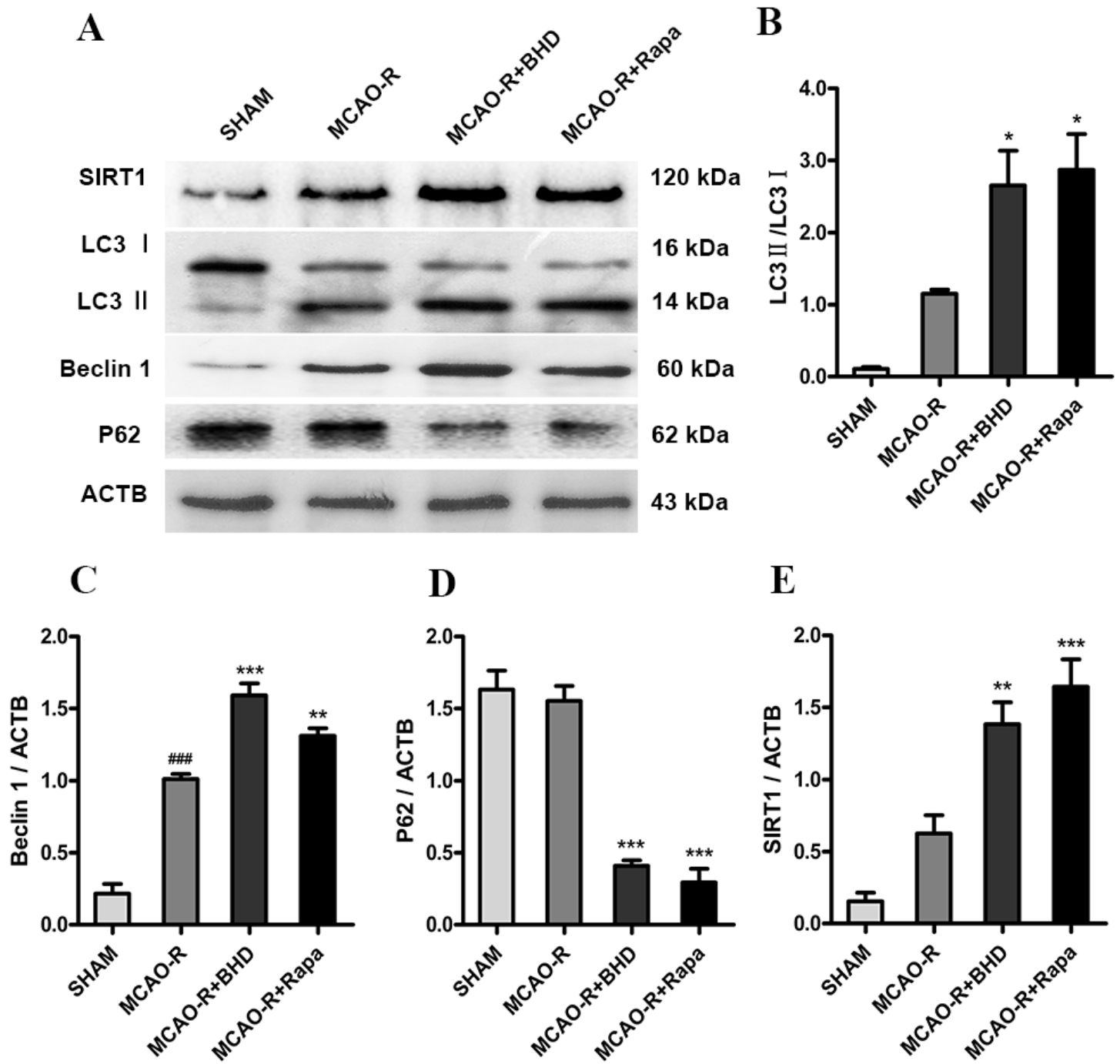


Figure 4

BHD activates SIRT1/autophagy of rat cerebral peri-ischemic area after MCAO-R. (A) Western blots of LC3, Beclin1, P62, SIRT1 in BHD-treated MCAO-R rats. (B-E) Quantitative analysis of the immunoblotted proteins was performed with Image J. Statistical comparisons were carried out with ANOVA followed by Tukey's test. Data are presented as means \pm SD (n = 3). #p < 0.05, ###p < 0.01, ###p < 0.001 vs. SHAM group; *p < 0.05, **p < 0.01, ***p < 0.001 vs. MCAO-R group.

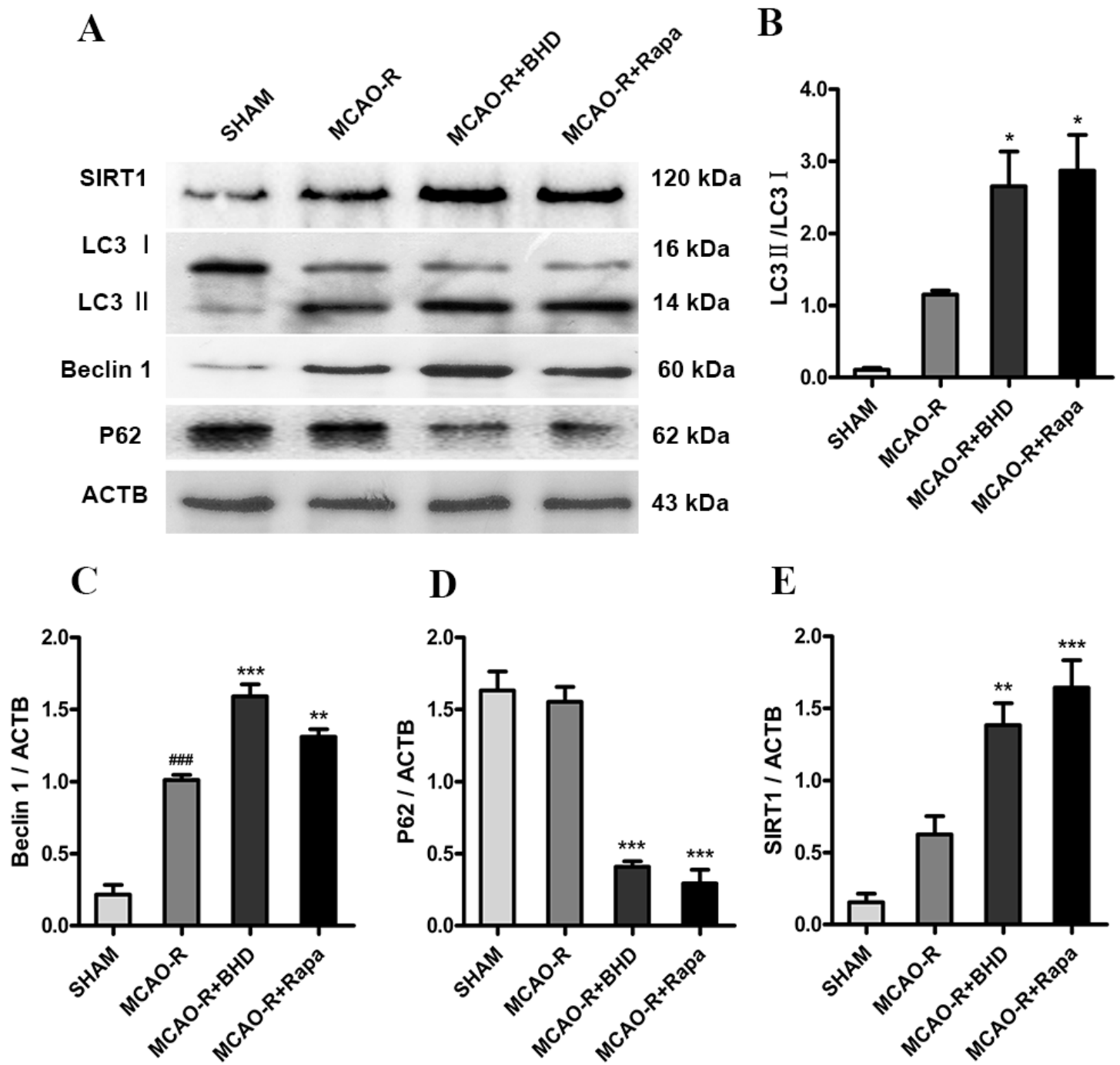


Figure 4

BHD activates SIRT1/autophagy of rat cerebral peri-ischemic area after MCAO-R. (A) Western blots of LC3, Beclin1, P62, SIRT1 in BHD-treated MCAO-R rats. (B-E) Quantitative analysis of the immunoblotted proteins was performed with Image J. Statistical comparisons were carried out with ANOVA followed by Tukey's test. Data are presented as means \pm SD (n = 3). #p < 0.05, ##p < 0.01, ###p < 0.001 vs. SHAM group; *p < 0.05, **p < 0.01, ***p < 0.001 vs. MCAO-R group.

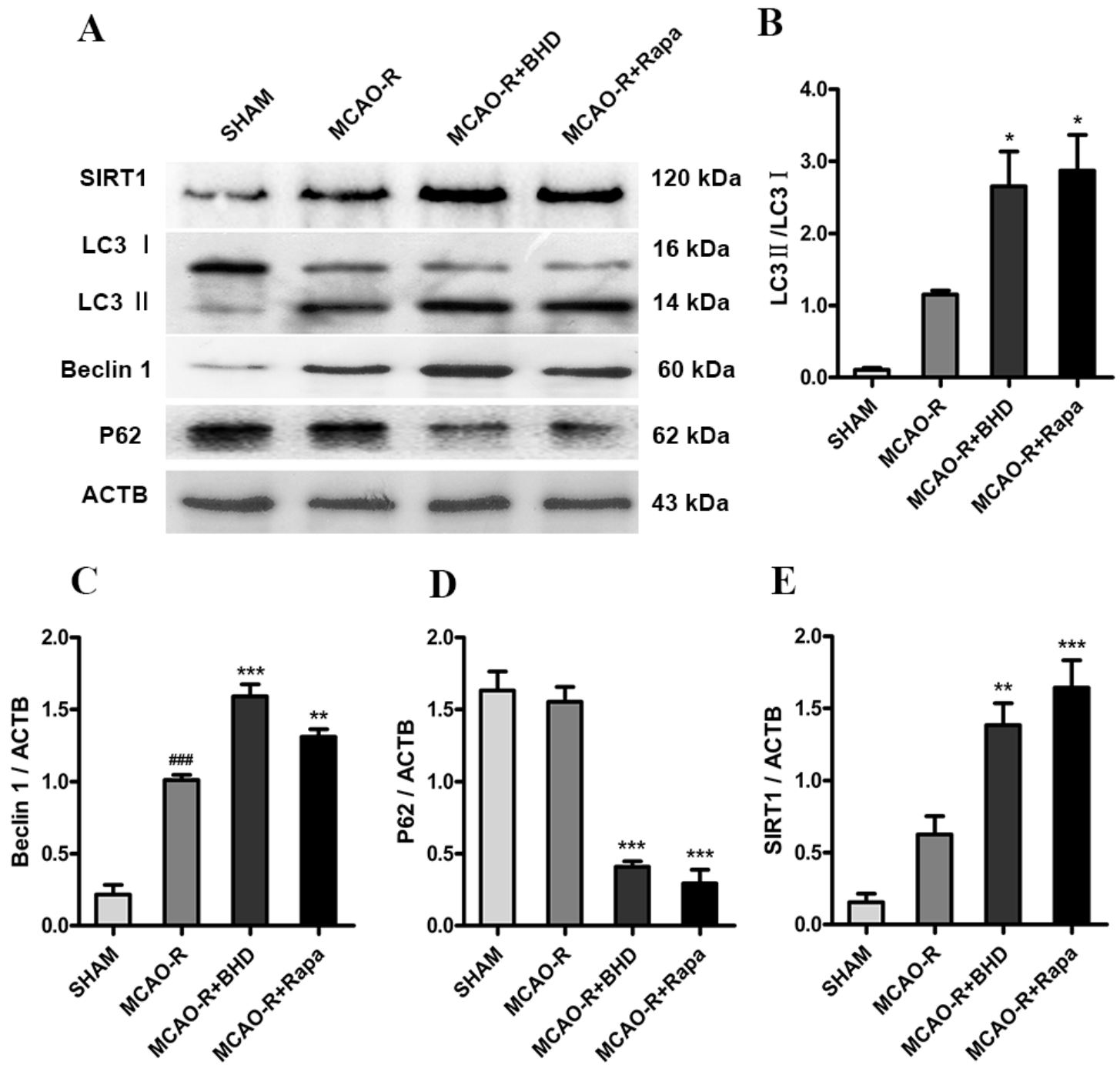


Figure 4

BHD activates SIRT1/autophagy of rat cerebral peri-ischemic area after MCAO-R. (A) Western blots of LC3, Beclin1, P62, SIRT1 in BHD-treated MCAO-R rats. (B-E) Quantitative analysis of the immunoblotted proteins was performed with Image J. Statistical comparisons were carried out with ANOVA followed by Tukey's test. Data are presented as means \pm SD (n = 3). #p < 0.05, ##p < 0.01, ###p < 0.001 vs. SHAM group; *p < 0.05, **p < 0.01, ***p < 0.001 vs. MCAO-R group.

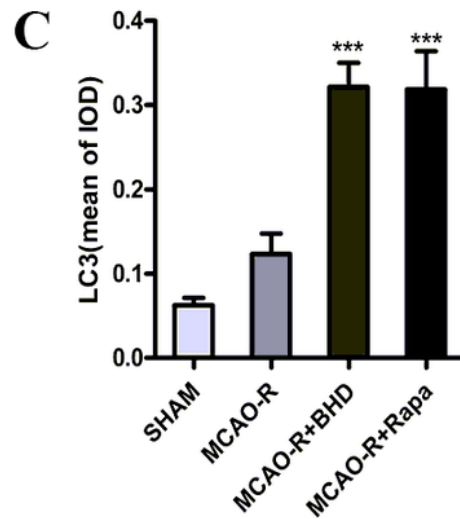
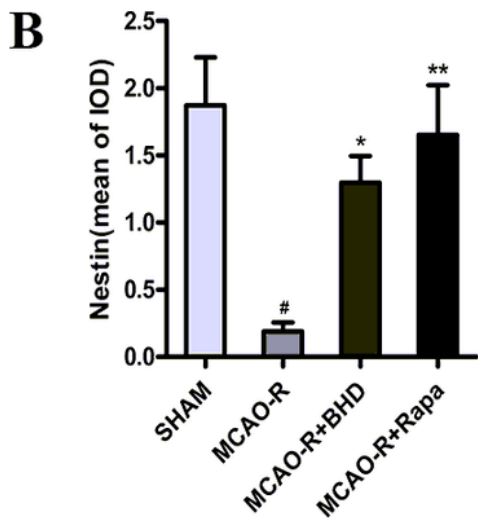
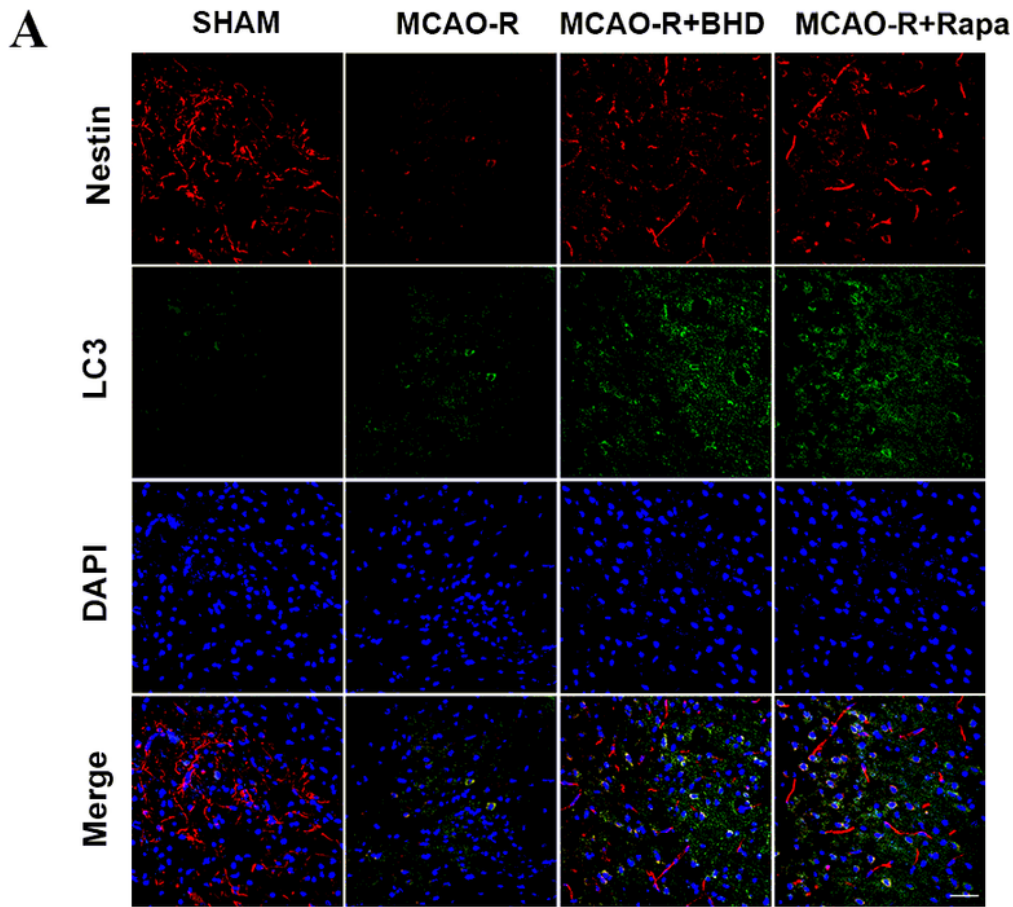


Figure 5

The BHD-induced neuroprotection is correlated with enhancement of autophagy. (A) The distribution of colocalization of nestin with the LC3 after MCAO-R in rat cerebral peri-ischemic area.

Immunofluorescence images showing the colocalization of Nestin (red) with LC3 (green). Nuclei were stained with DAPI (blue). Scale bar: 10 μ m. (B and C) The immunofluorescence intensity of Nestin and LC3. The data are expressed as means \pm SD (n = 3). Statistical comparisons were performed with one-

way ANOVA followed by Dunnett's t test. # $p < 0.05$, ## $p < 0.01$, ### $p < 0.001$ vs. SHAM group; * $p < 0.05$, ** $p < 0.01$, *** $p < 0.001$ vs. MCAO-R group.

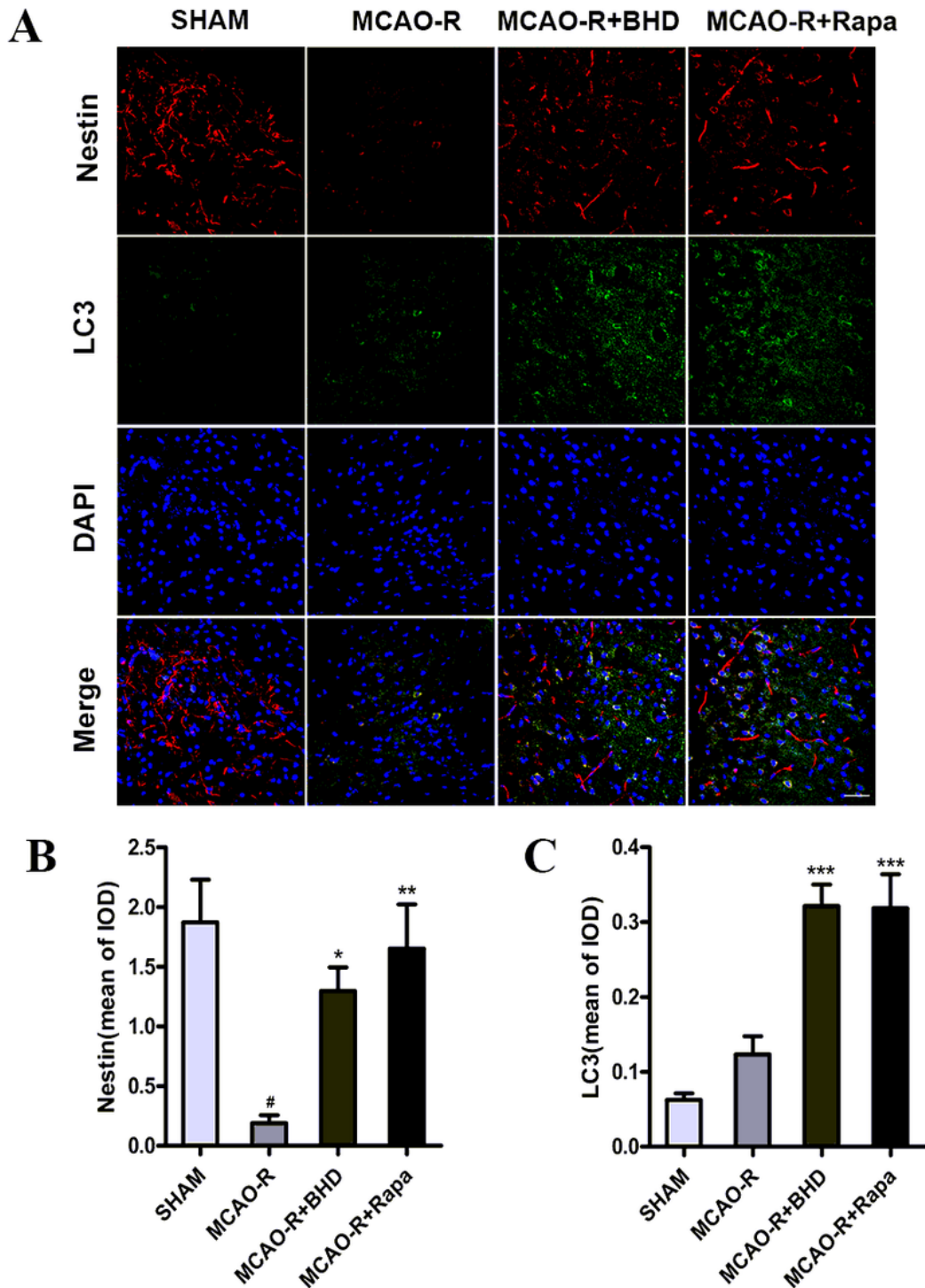


Figure 5

The BHD-induced neuroprotection is correlated with enhancement of autophagy. (A) The distribution of colocalization of nestin with the LC3 after MCAO-R in rat cerebral peri-ischemic area. Immunofluorescence images showing the colocalization of Nestin (red) with LC3 (green). Nuclei were

stained with DAPI (blue). Scale bar: 10 μ m. (B and C) The immunofluorescence intensity of Nestin and LC3. The data are expressed as means \pm SD (n = 3). Statistical comparisons were performed with one-way ANOVA followed by Dunnett's t test. #p < 0.05, ##p < 0.01, ###p < 0.001 vs. SHAM group; *p < 0.05, **p < 0.01, ***p < 0.001 vs. MCAO-R group.

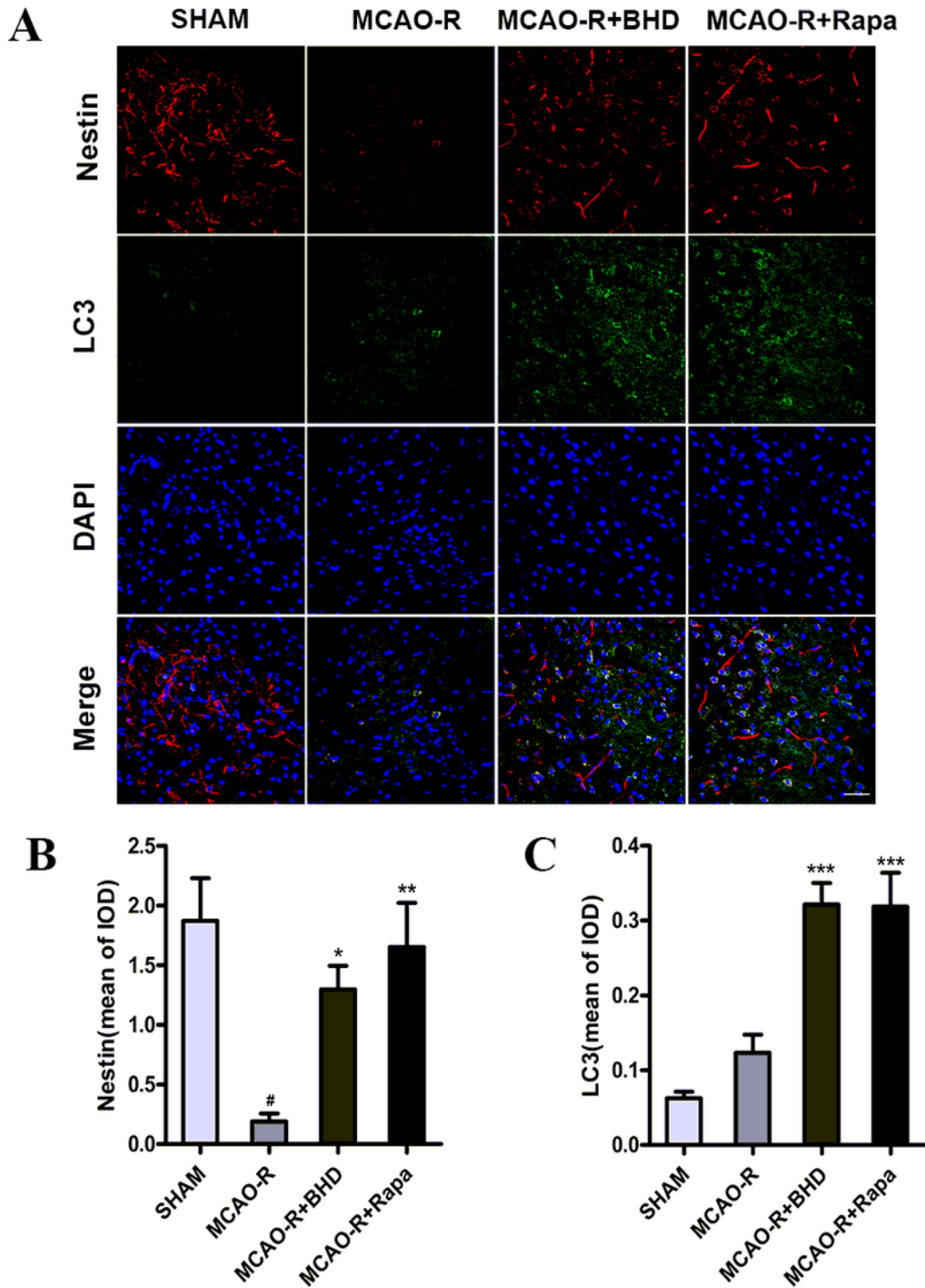


Figure 5

The BHD-induced neuroprotection is correlated with enhancement of autophagy. (A) The distribution of colocalization of nestin with the LC3 after MCAO-R in rat cerebral peri-ischemic area. Immunofluorescence images showing the colocalization of Nestin (red) with LC3 (green). Nuclei were stained with DAPI (blue). Scale bar: 10 μ m. (B and C) The immunofluorescence intensity of Nestin and LC3. The data are expressed as means \pm SD (n = 3). Statistical comparisons were performed with one-way ANOVA followed by Dunnett's t test. #p < 0.05, ##p < 0.01, ###p < 0.001 vs. SHAM group; *p < 0.05, **p < 0.01, ***p < 0.001 vs. MCAO-R group.

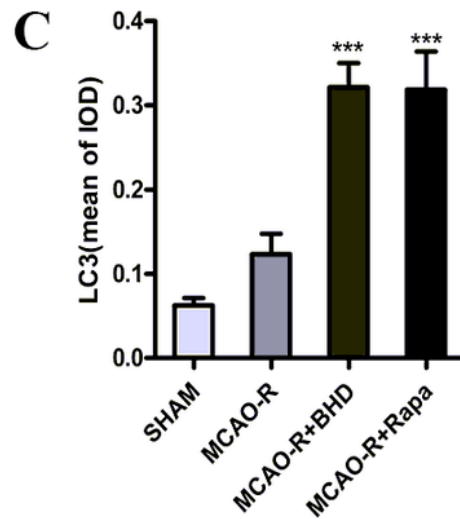
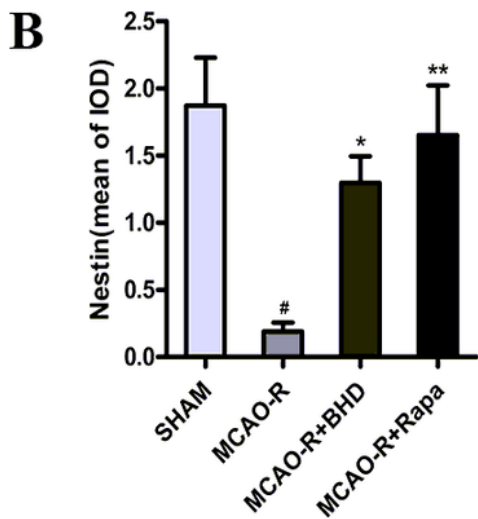
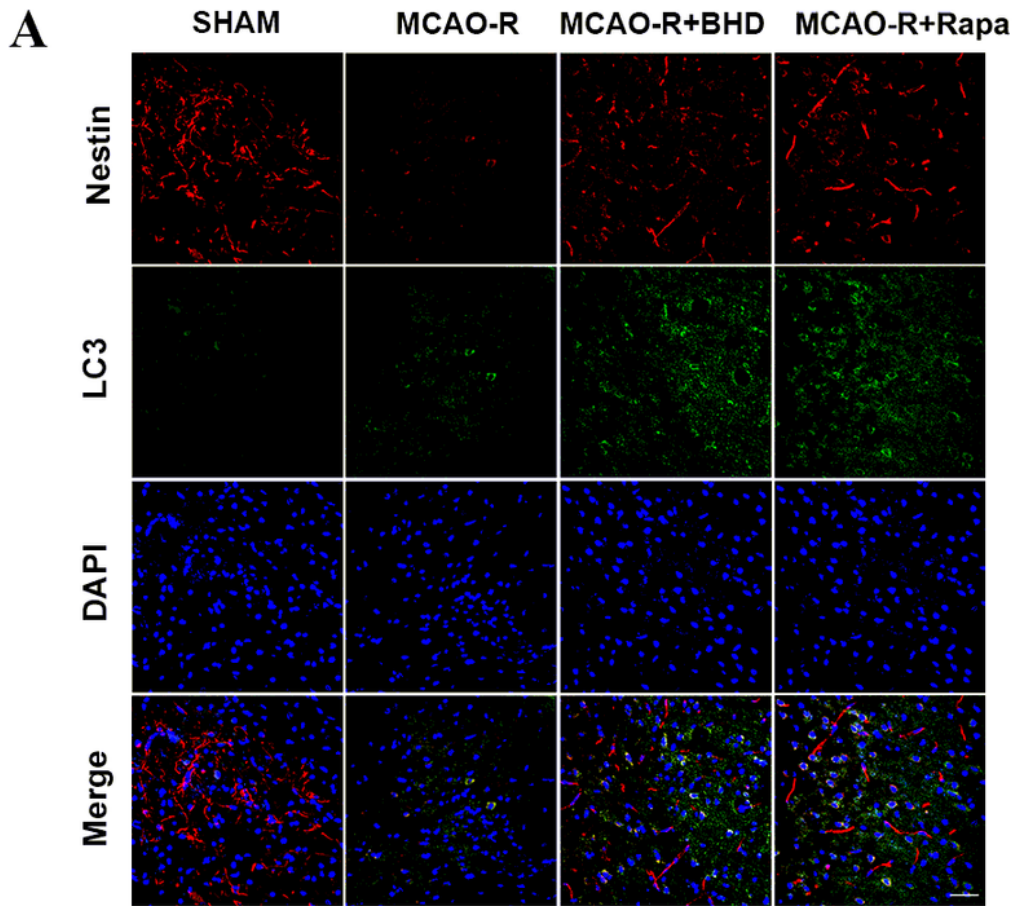
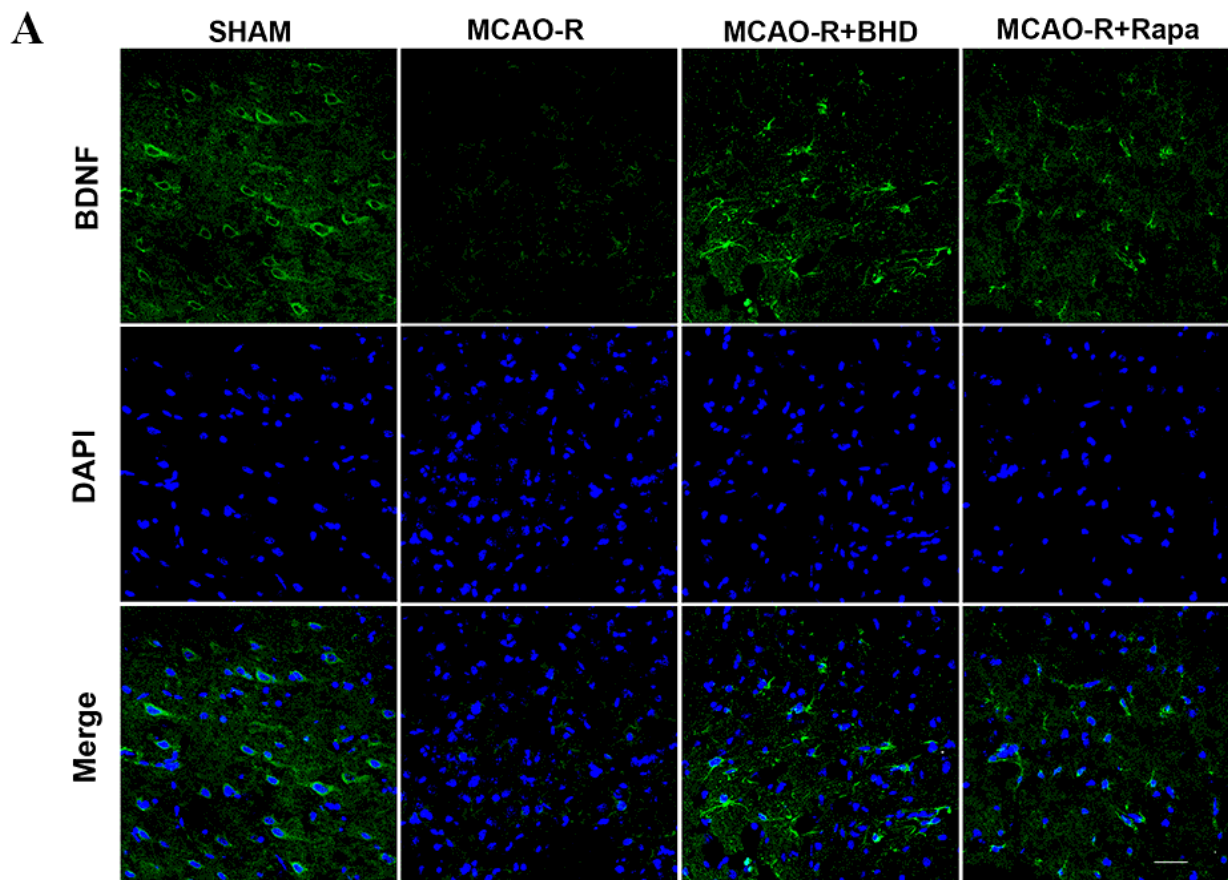


Figure 5

The BHD-induced neuroprotection is correlated with enhancement of autophagy. (A) The distribution of colocalization of nestin with the LC3 after MCAO-R in rat cerebral peri-ischemic area.

Immunofluorescence images showing the colocalization of Nestin (red) with LC3 (green). Nuclei were stained with DAPI (blue). Scale bar: 10 μ m. (B and C) The immunofluorescence intensity of Nestin and LC3. The data are expressed as means \pm SD (n = 3). Statistical comparisons were performed with one-way ANOVA followed by Dunnett's t test. #p < 0.05, ##p < 0.01, ###p < 0.001 vs. SHAM group; *p < 0.05, **p < 0.01, ***p < 0.001 vs. MCAO-R group.



B

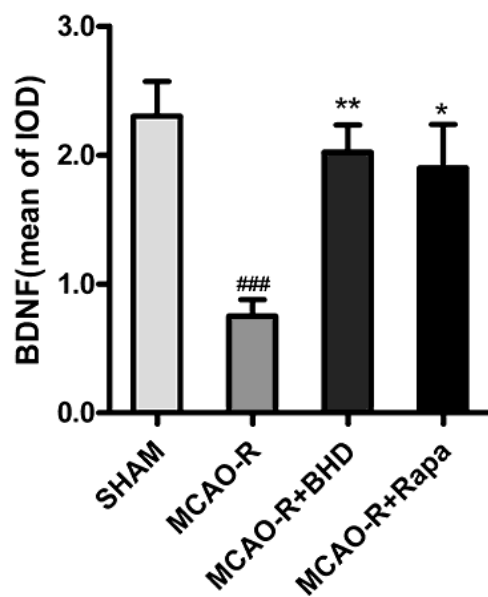


Figure 6

BHD produces neuroprotection in rat cerebral peri-ischemic area after MCAO-R. (A) IF analysis performed with brain-derived neurotrophic factor (BDNF) antibody (green), nuclei were stained with DAPI (blue). Scale bar: 10 μ m. (B) The bar graph represents the IOD quantification of BDNF. The data are expressed as means \pm SD (n = 3). Statistical comparisons were performed with one-way ANOVA followed by Dunnett's t

test. #p < 0.05, ##p < 0.01, ###p < 0.001 vs. SHAM group; *p < 0.05, **p < 0.01, ***p < 0.001 vs. MCAO-R group.

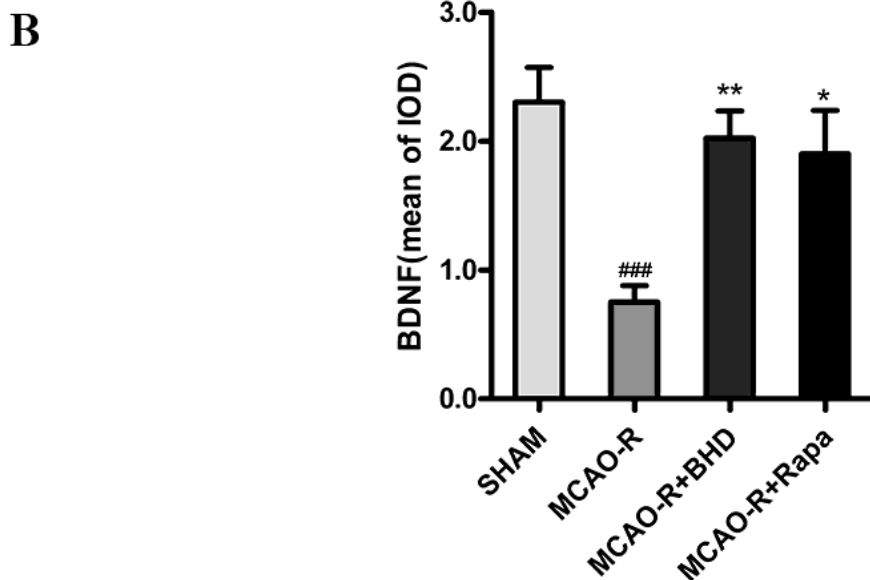
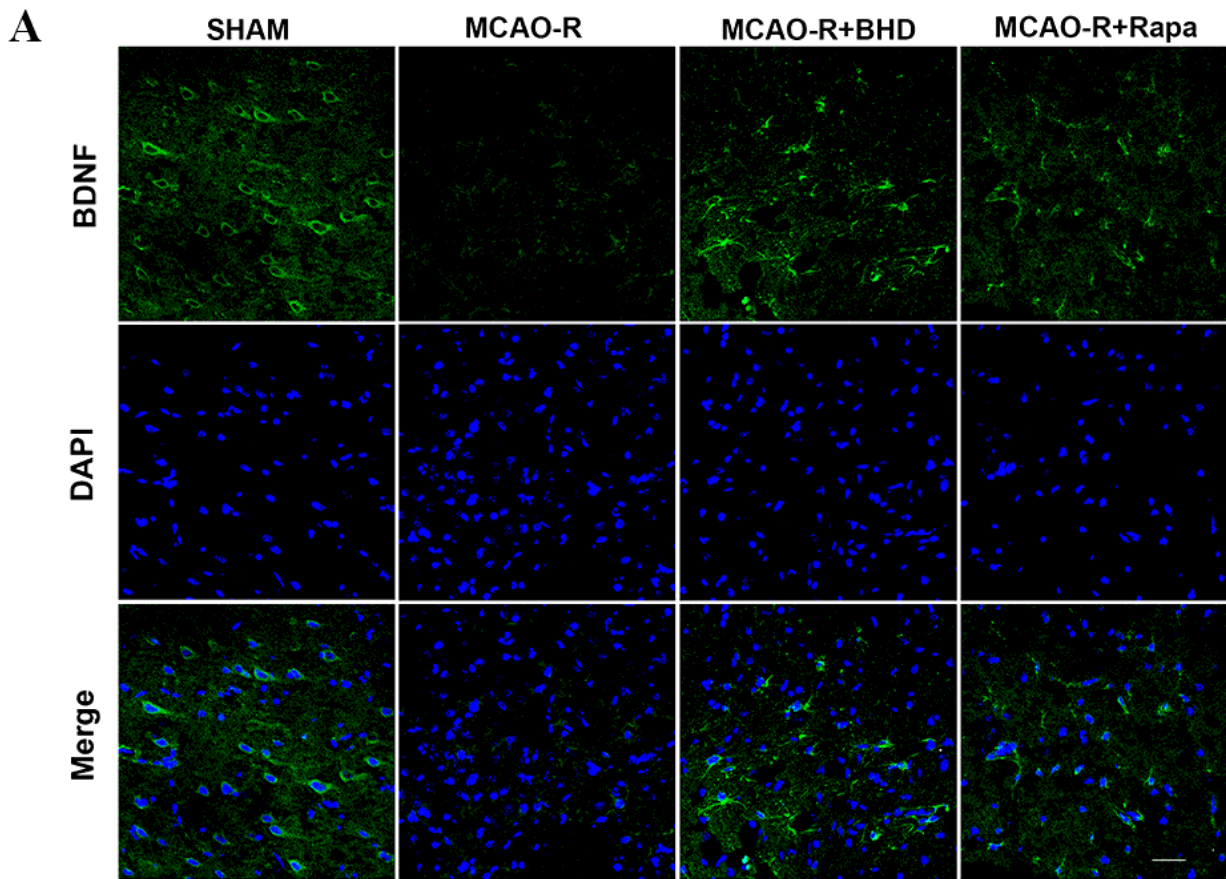


Figure 6

BHD produces neuroprotection in rat cerebral peri-ischemic area after MCAO-R. (A) IF analysis performed with brain-derived neurotrophic factor (BDNF) antibody (green), nuclei were stained with DAPI (blue). Scale bar: 10 μ m. (B) The bar graph represents the IOD quantification of BDNF. The data are expressed as

means \pm SD (n = 3). Statistical comparisons were performed with one-way ANOVA followed by Dunnett's t test. #p < 0.05, ##p < 0.01, ###p < 0.001 vs. SHAM group; *p < 0.05, **p < 0.01, ***p < 0.001 vs. MCAO-R group.

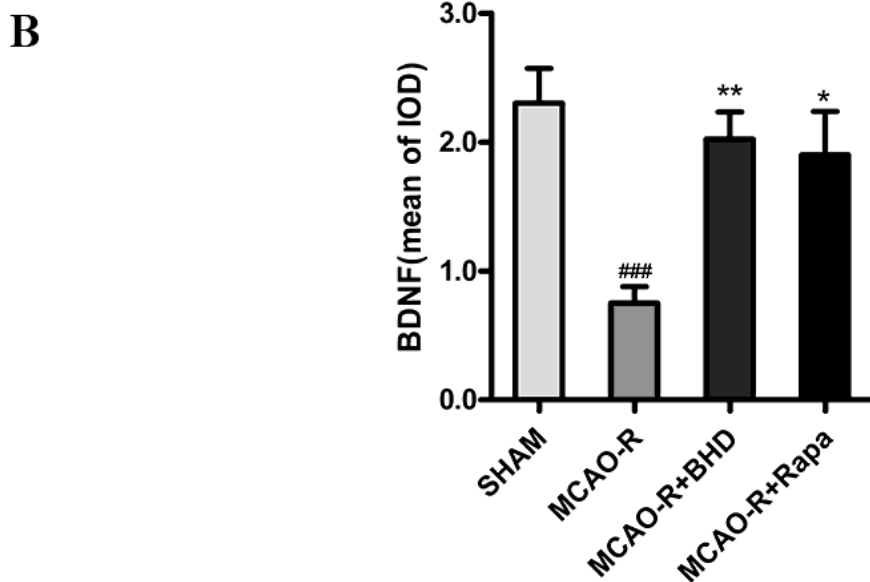
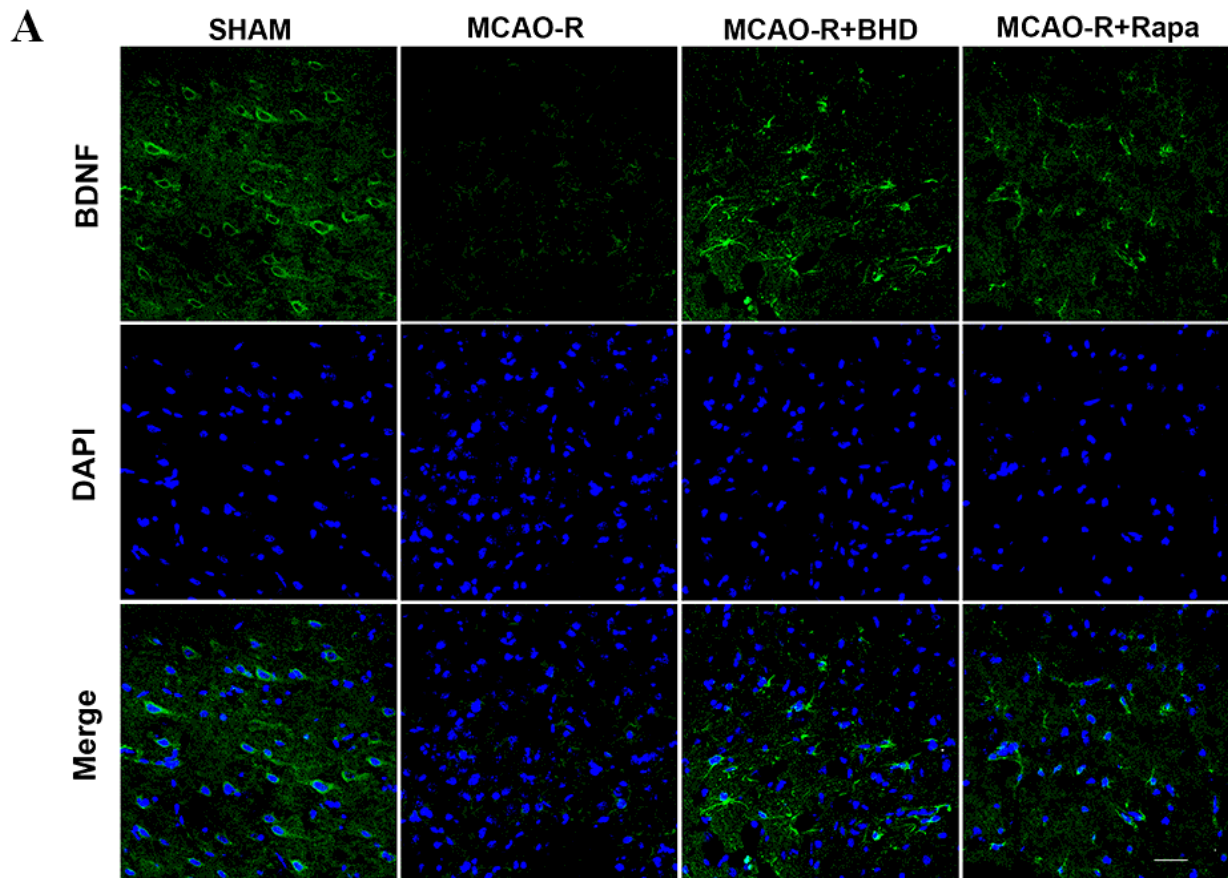


Figure 6

BHD produces neuroprotection in rat cerebral peri-ischemic area after MCAO-R. (A) IF analysis performed with brain-derived neurotrophic factor (BDNF) antibody (green), nuclei were stained with DAPI (blue).

Scale bar: 10 μ m. (B) The bar graph represents the IOD quantification of BDNF. The data are expressed as means \pm SD (n = 3). Statistical comparisons were performed with one-way ANOVA followed by Dunnett's t test. #p < 0.05, ##p < 0.01, ###p < 0.001 vs. SHAM group; *p < 0.05, **p < 0.01, ***p < 0.001 vs. MCAO-R group.

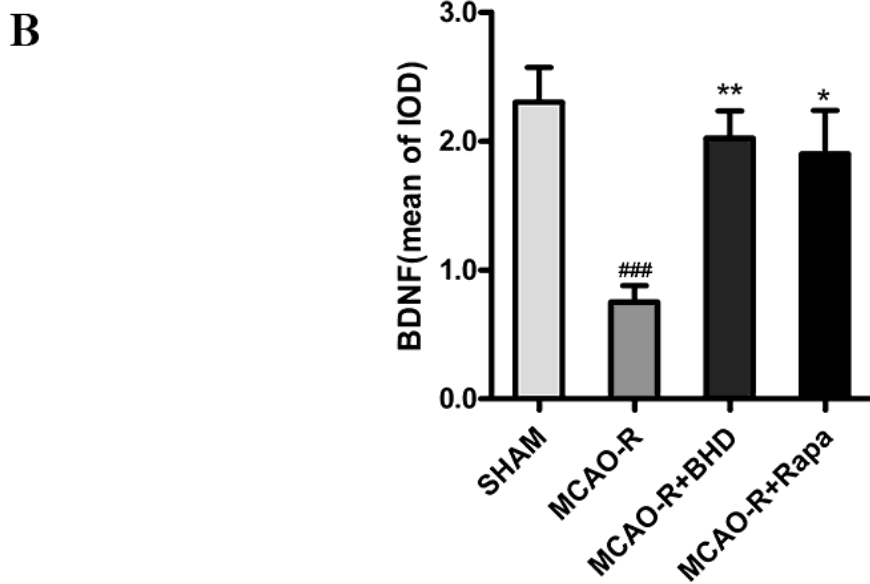
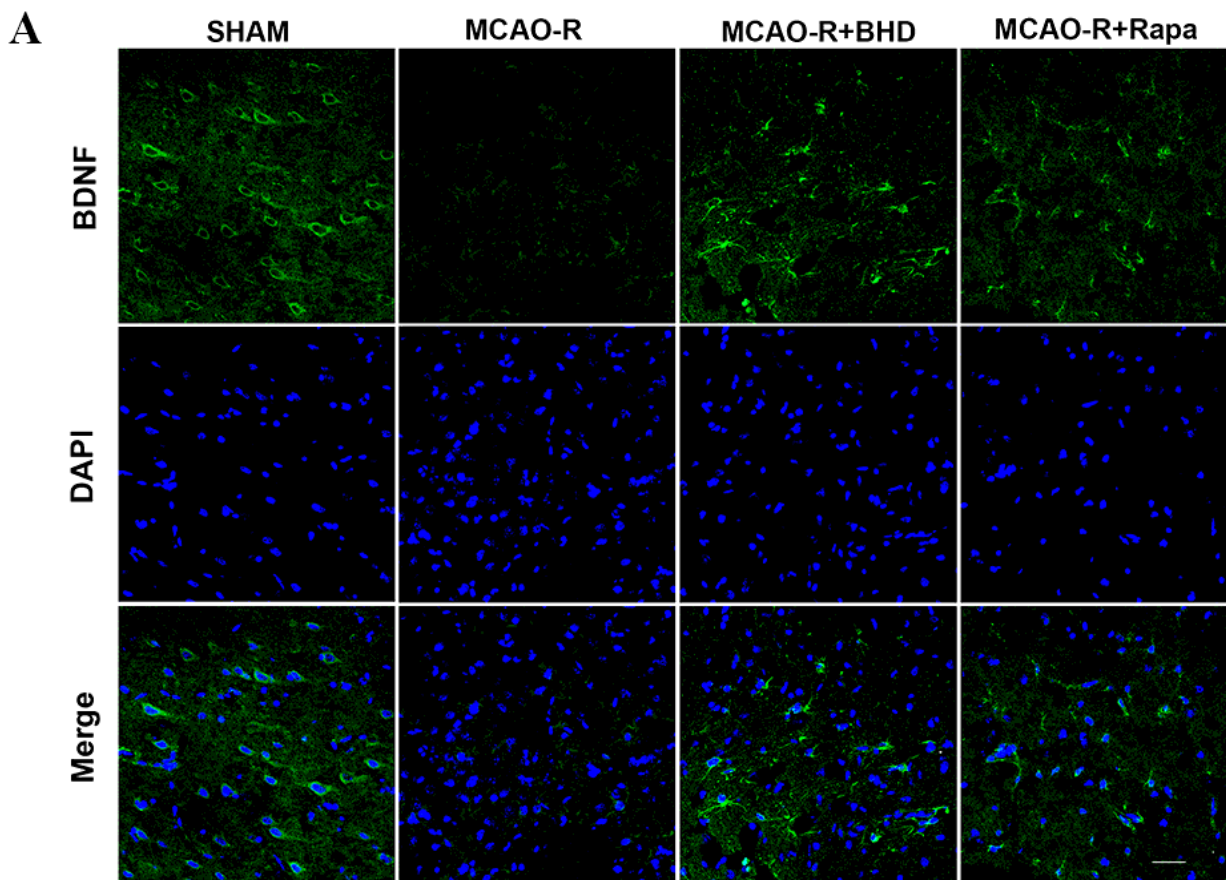


Figure 6

BHD produces neuroprotection in rat cerebral peri-ischemic area after MCAO-R. (A) IF analysis performed with brain-derived neurotrophic factor (BDNF) antibody (green), nuclei were stained with DAPI (blue). Scale bar: 10 μ m. (B) The bar graph represents the IOD quantification of BDNF. The data are expressed as means \pm SD (n = 3). Statistical comparisons were performed with one-way ANOVA followed by Dunnett's t test. #p < 0.05, ##p < 0.01, ###p < 0.001 vs. SHAM group; *p < 0.05, **p < 0.01, ***p < 0.001 vs. MCAO-R group.

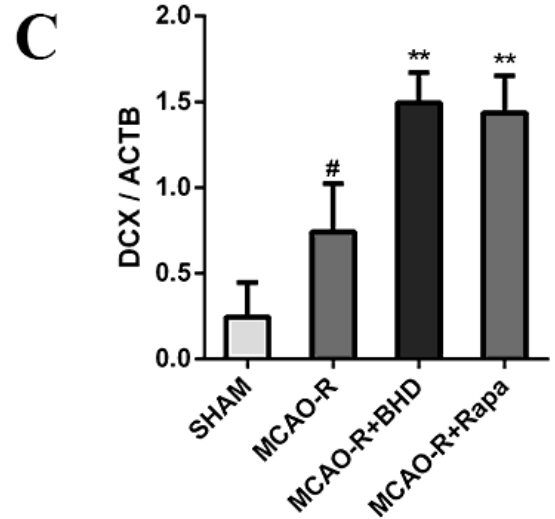
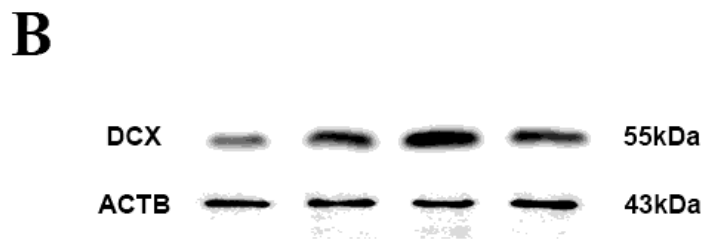
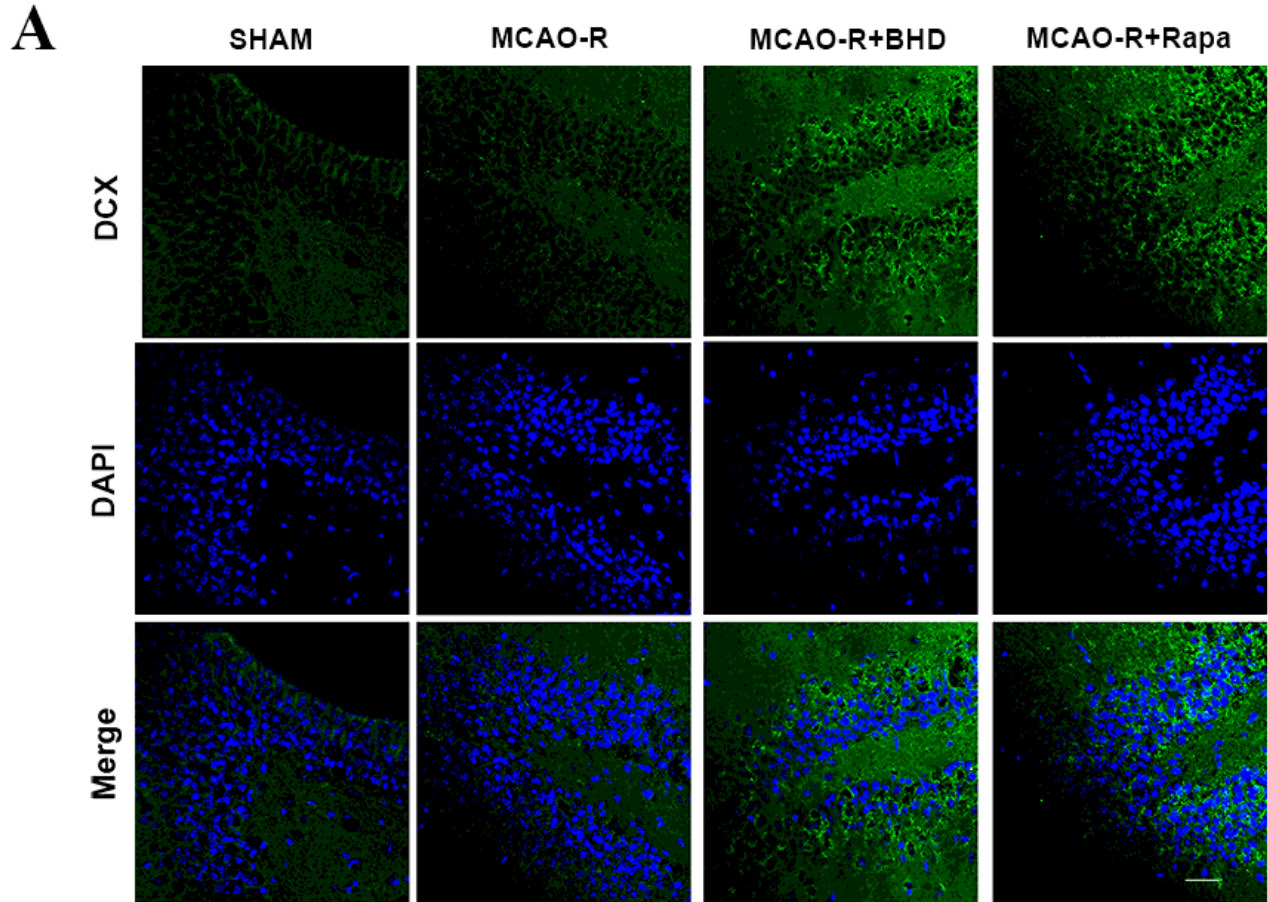


Figure 7

BHD promotes neurogenesis after MCAO-R. (A) IF analysis performed with Doublecortin on the X-chromosome (DCX) positive cells in the subgranular zone of the hippocampal dentate gyrus of rats (green), nuclei were stained with DAPI (blue). Scale bar: 10 μ m. (B and C) Quantification of DCX by western blot. The data are expressed as means \pm SD (n = 3). Statistical comparisons were performed with one-way ANOVA followed by Dunnett's t test. #p < 0.05, ##p < 0.01, ###p < 0.001 vs. SHAM group; *p < 0.05, **p < 0.01, ***p < 0.001 vs. MCAO-R group.

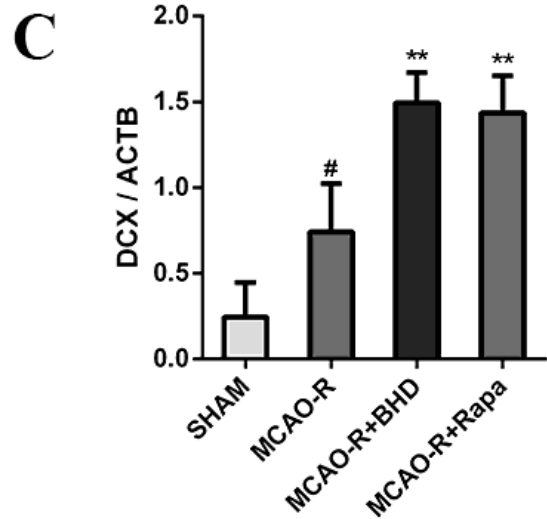
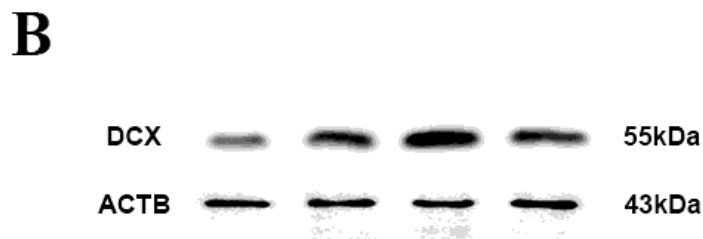
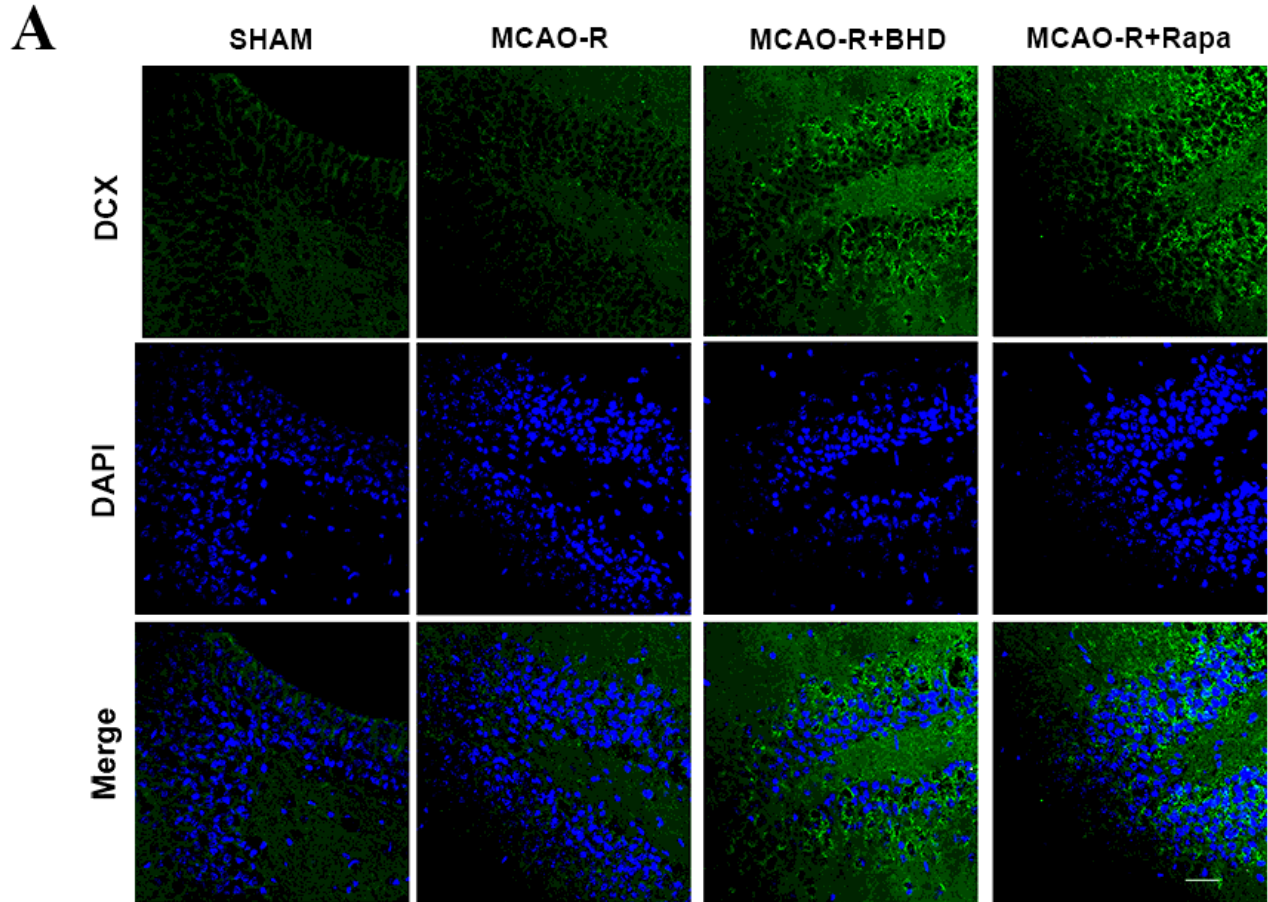


Figure 7

BHD promotes neurogenesis after MCAO-R. (A) IF analysis performed with Doublecortin on the X-chromosome (DCX) positive cells in the subgranular zone of the hippocampal dentate gyrus of rats (green), nuclei were stained with DAPI (blue). Scale bar: 10 μ m. (B and C) Quantification of DCX by western blot. The data are expressed as means \pm SD (n = 3). Statistical comparisons were performed with one-way ANOVA followed by Dunnett's t test. #p < 0.05, ##p < 0.01, ###p < 0.001 vs. SHAM group; *p < 0.05, **p < 0.01, ***p < 0.001 vs. MCAO-R group.

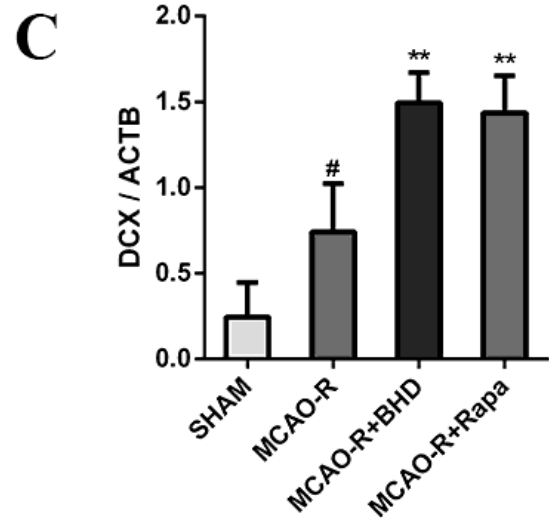
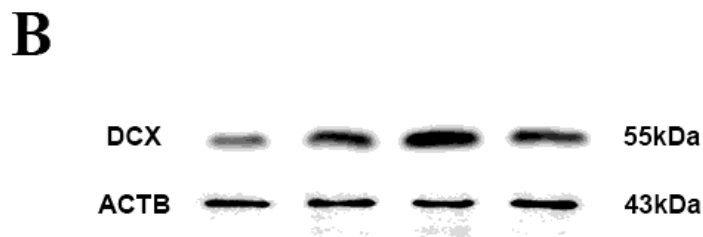
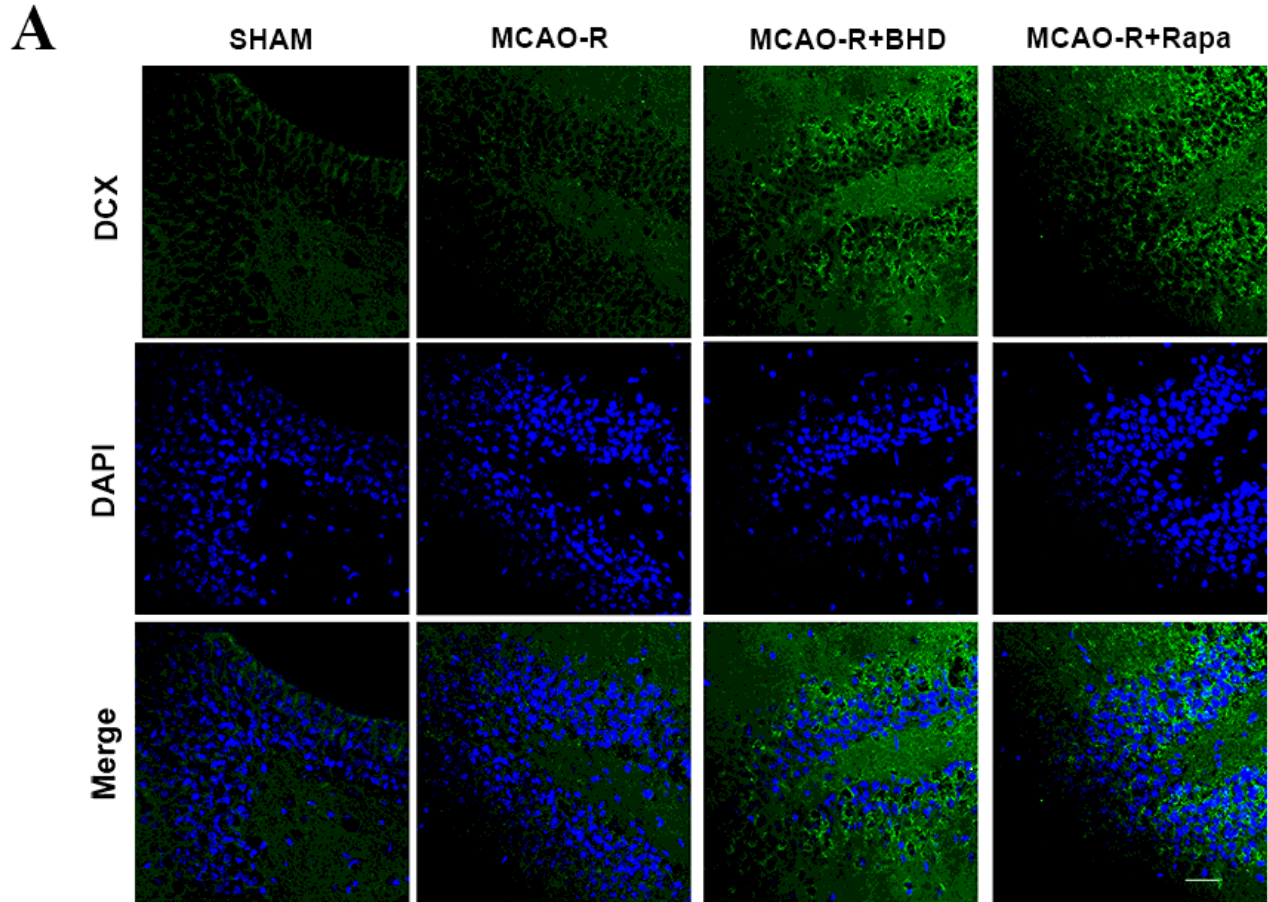


Figure 7

BHD promotes neurogenesis after MCAO-R. (A) IF analysis performed with Doublecortin on the X-chromosome (DCX) positive cells in the subgranular zone of the hippocampal dentate gyrus of rats (green), nuclei were stained with DAPI (blue). Scale bar: 10 μ m. (B and C) Quantification of DCX by western blot. The data are expressed as means \pm SD (n = 3). Statistical comparisons were performed with one-way ANOVA followed by Dunnett's t test. #p < 0.05, ##p < 0.01, ###p < 0.001 vs. SHAM group; *p < 0.05, **p < 0.01, ***p < 0.001 vs. MCAO-R group.

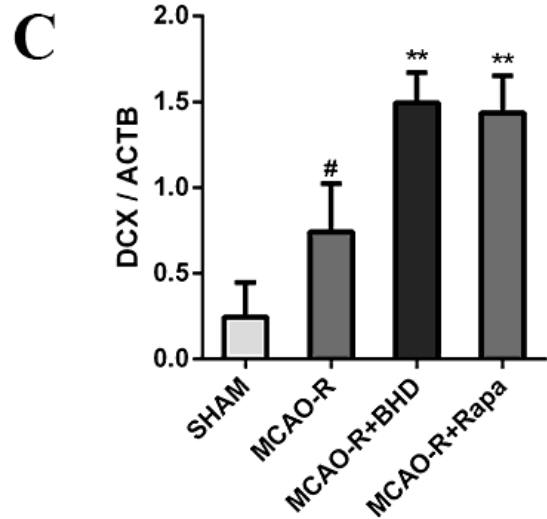
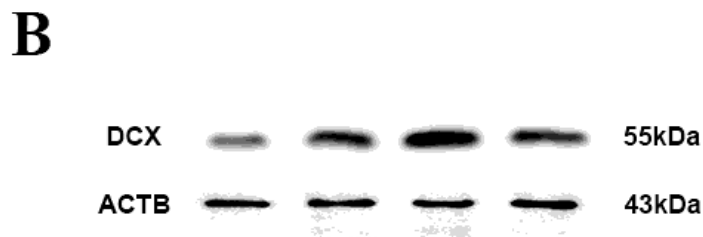
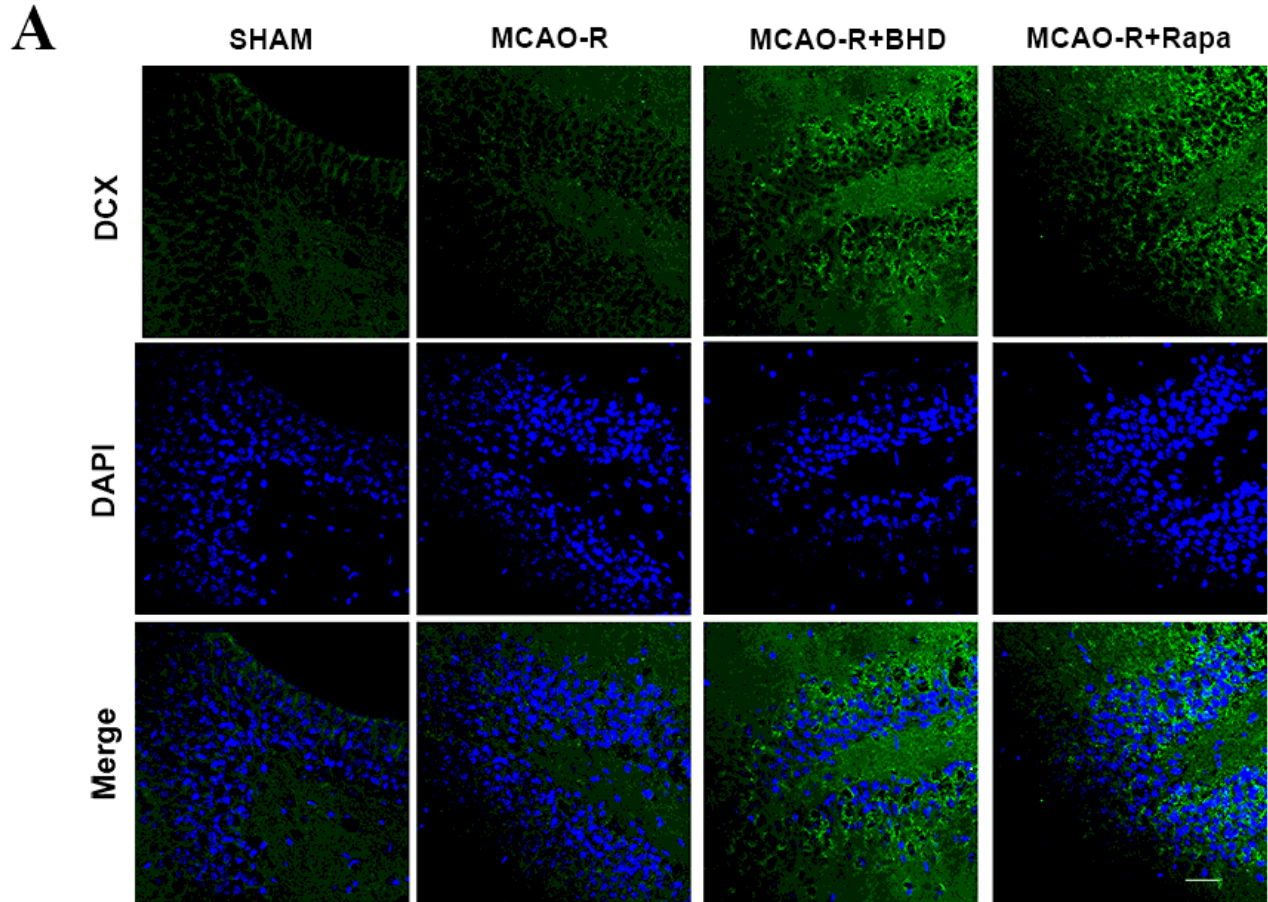


Figure 7

BHD promotes neurogenesis after MCAO-R. (A) IF analysis performed with Doublecortin on the X-chromosome (DCX) positive cells in the subgranular zone of the hippocampal dentate gyrus of rats (green), nuclei were stained with DAPI (blue). Scale bar: 10 μ m. (B and C) Quantification of DCX by western blot. The data are expressed as means \pm SD (n = 3). Statistical comparisons were performed with one-way ANOVA followed by Dunnett's t test. #p < 0.05, ##p < 0.01, ###p < 0.001 vs. SHAM group; *p < 0.05, **p < 0.01, ***p < 0.001 vs. MCAO-R group.